The Universe in X-rays:

Overview of HW#4

Energy dependent characteristic of X-ray satellites

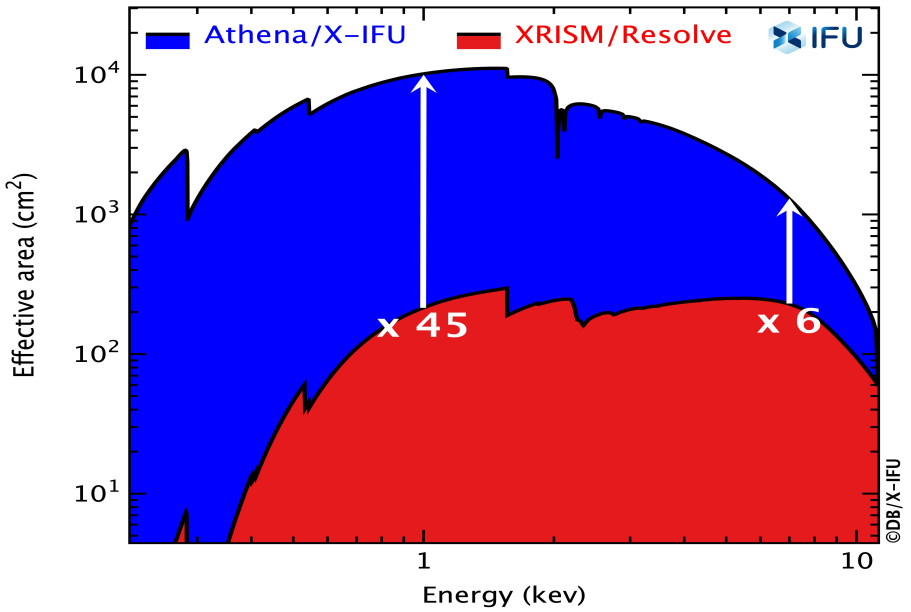

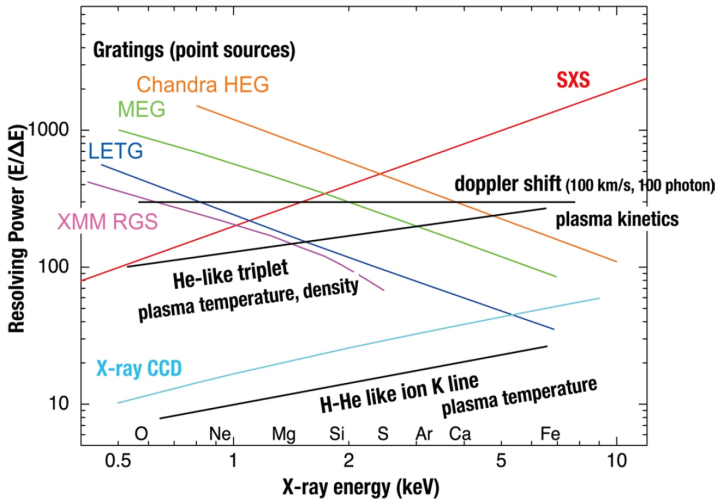

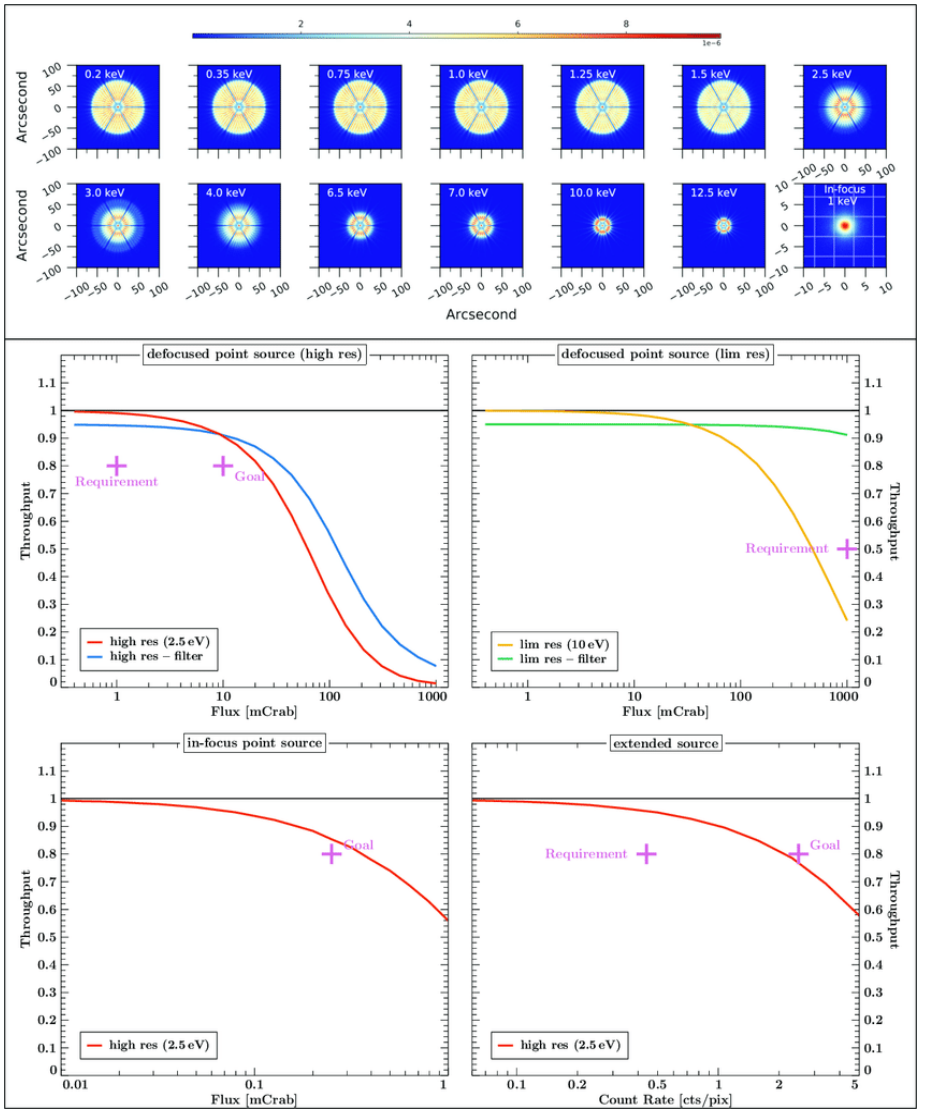

Time resolution

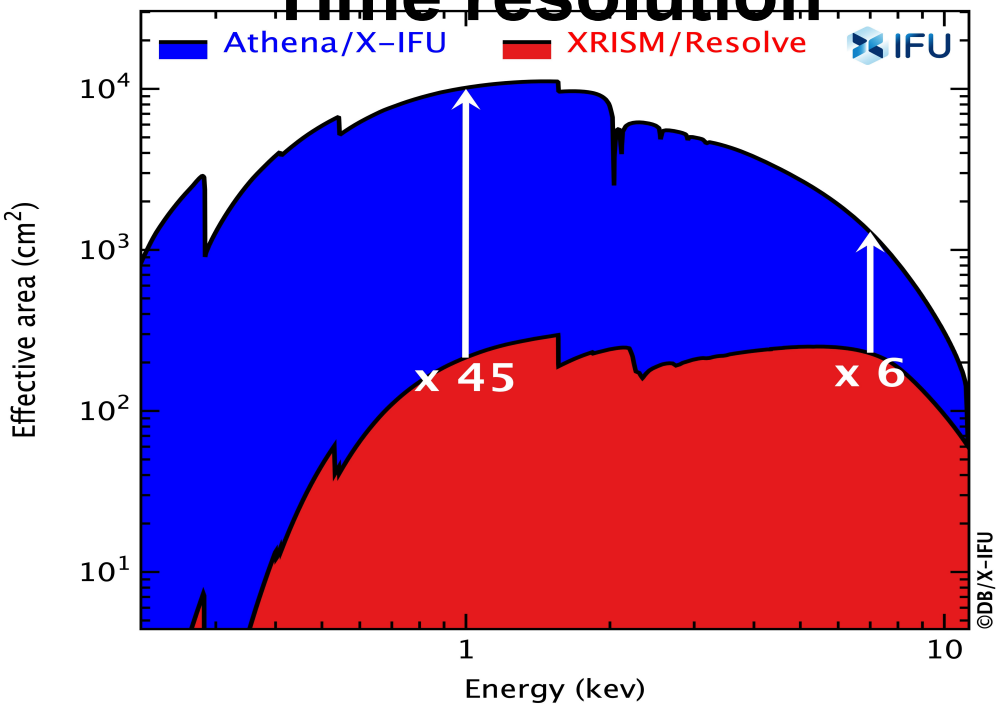

Energy resolution

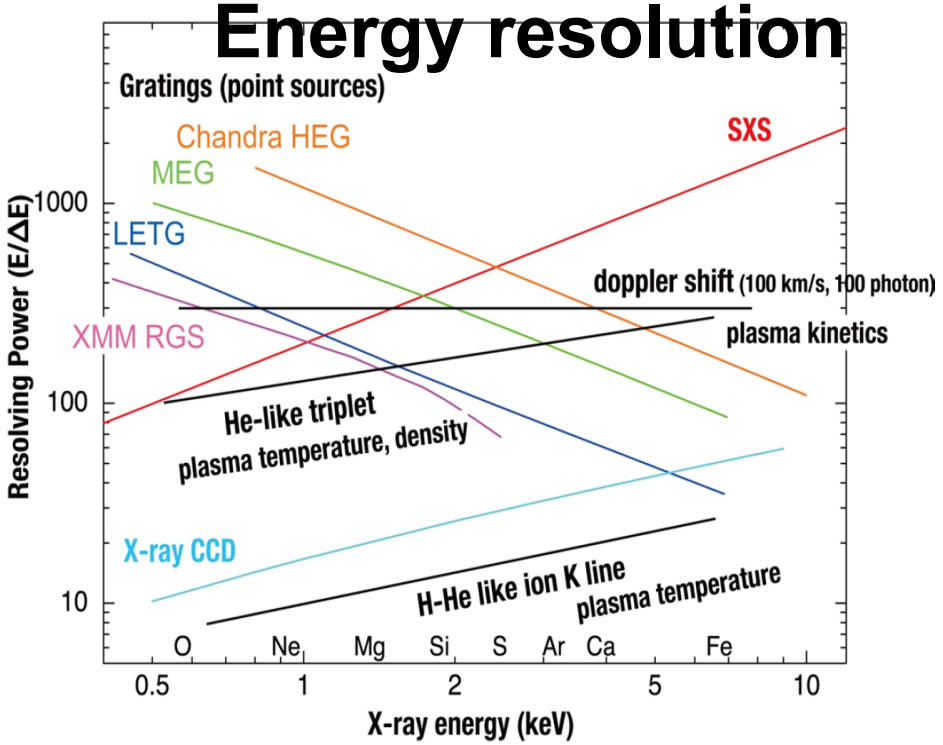

Spacial resolution

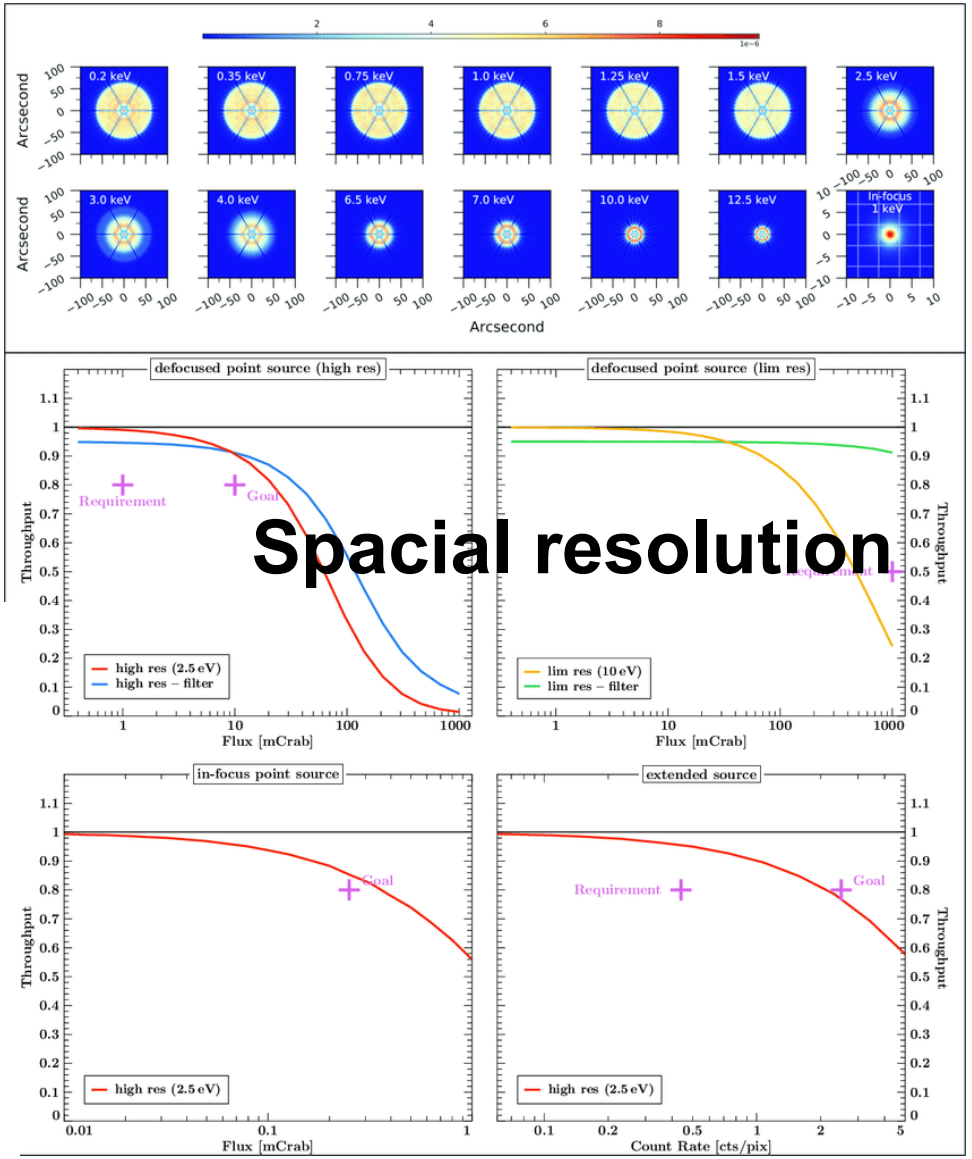

Energy resolution

EXOSAT mission:

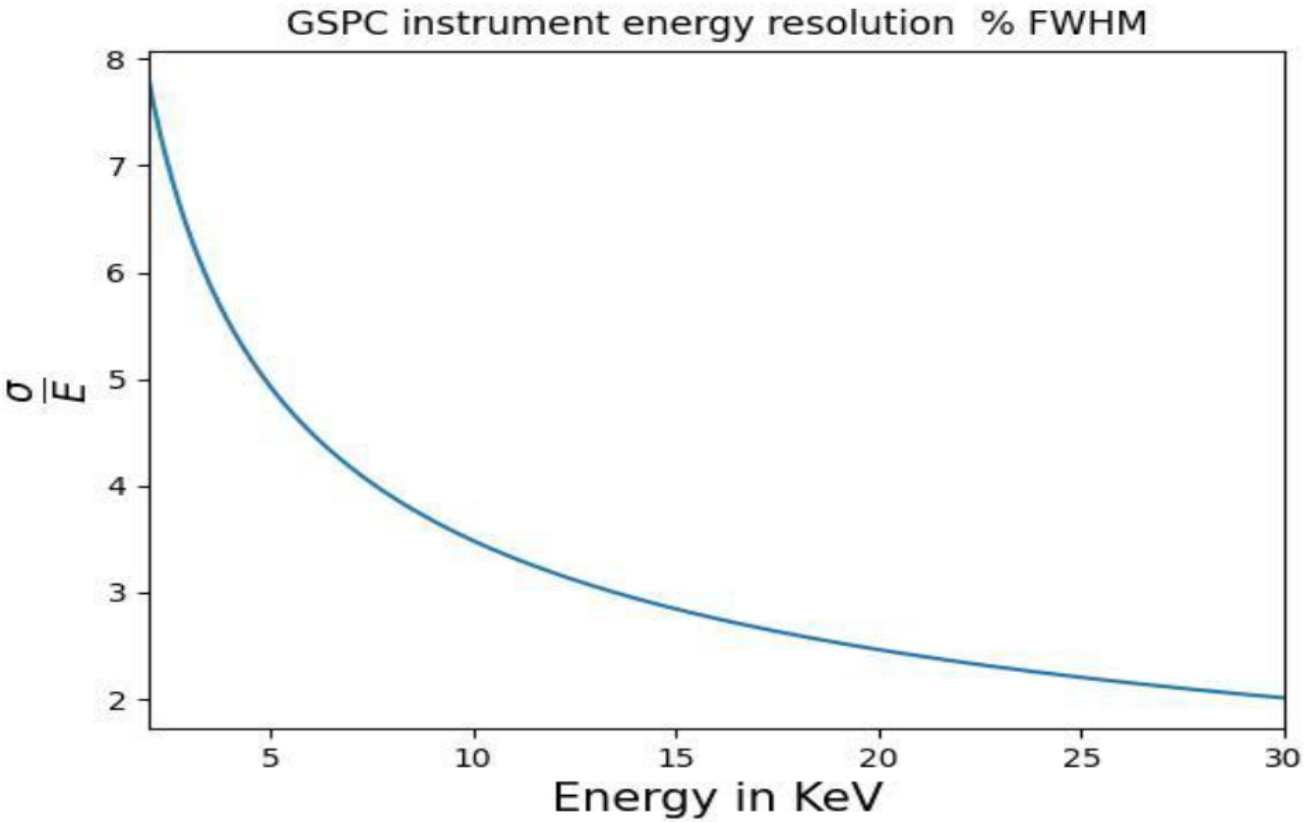

deltaE/E of $4.5(E/6\ keV)^{-0.5}$ % FWHM

Energy resolution

EXOSAT mission:

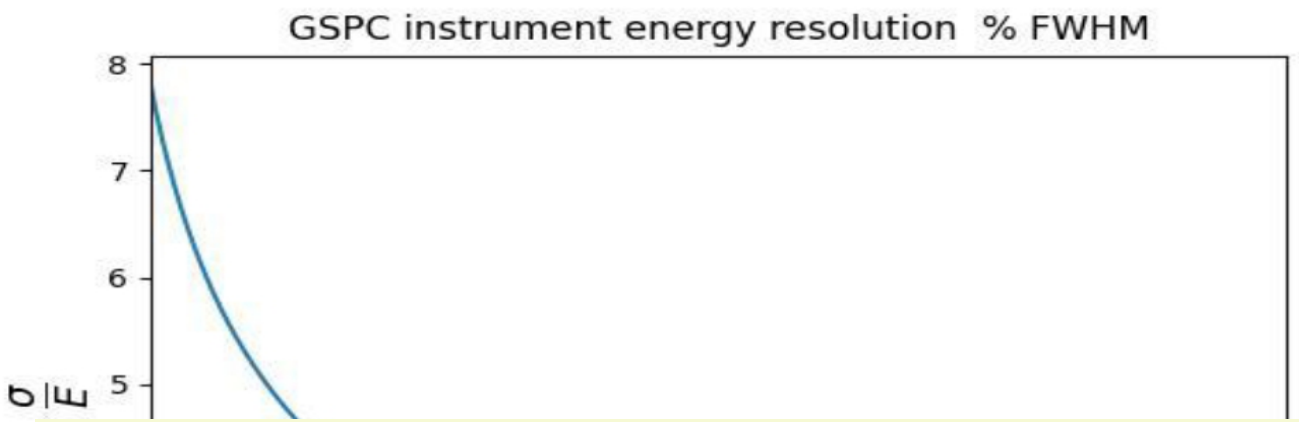

HW4 : NuSTAR – Energy Resolution
Sudhagar Suyamprakasam, CAMK- PAN

Focal plane CdZnTe detectors (2x2 array/module)

• Size	2 x 2 cm
• Physical pixel number	32 x 32
• Pixel pitch	604.8 µm
• Sky plate scale	2.45 arcsec
• Maximum readout rate	400 events s -1
• Energy range	3 to 78.4 keV
• Spectral resolution	400 / 900 eV at 10 / 68 keV
• Temporal resolution	2 x 10 -3 s (RMS)

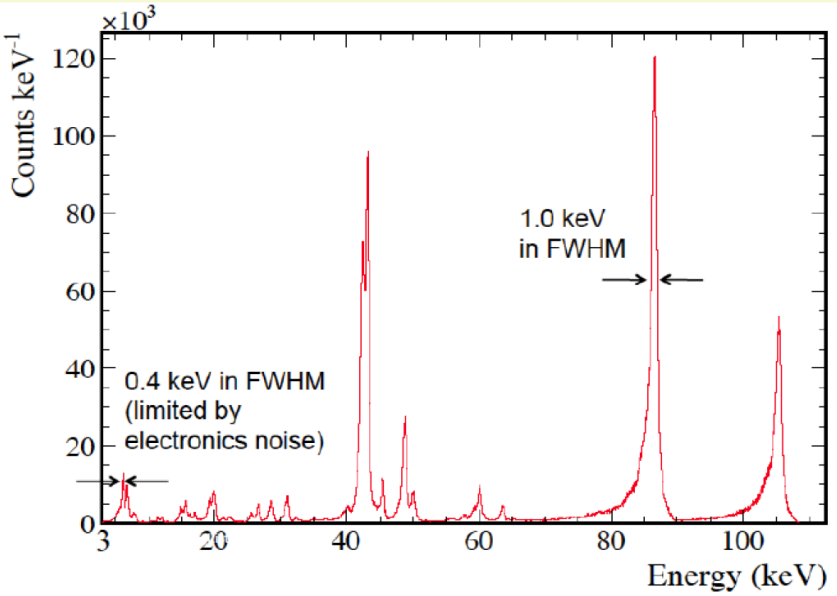

Inflight spectrum of the FPMB/DET0 detector irradiated with the onboard 155Eu radioactive source. The energy resolution (FWHM) is 0.4 keV below 50 keV and rises to 1.0 keV at 86 keV.

Energy resolution

EXOSAT mission:

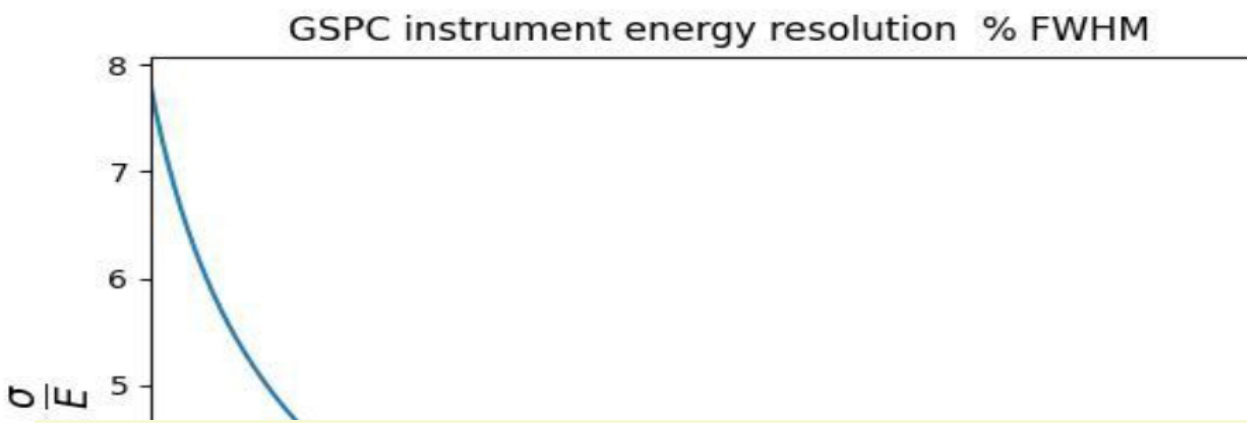

ATHENA

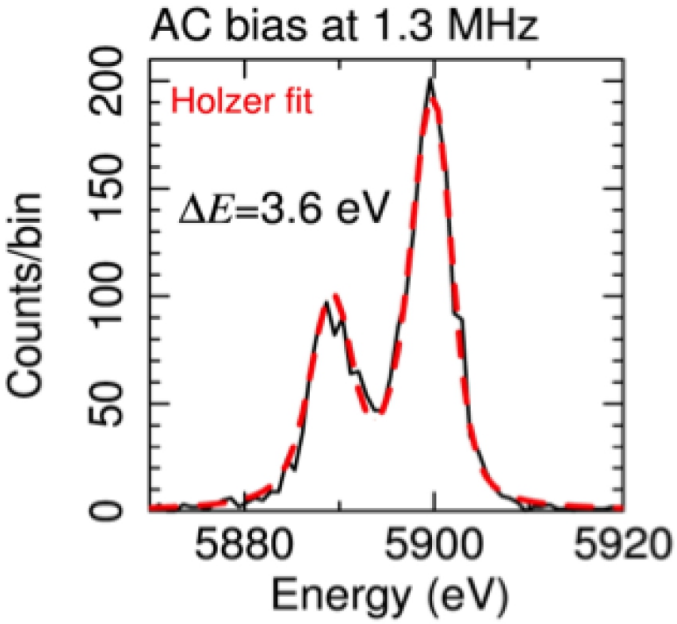

HW4 : NuSTAR – Energy Resol
Sudhagar Suyamprakasam, CAM

Focal plane CdZnTe detectors (2x2 array/module)

• Size	2 x 2 cm
• Physical pixel number	32 x 32
• Pixel pitch	604.8 µm
• Sky plate scale	2.45 arcsec
• Maximum readout rate	400 events s -1
• Energy range	3 to 78.4 keV
• Spectral resolution	400 / 900 eV at 10 / 68 keV
• Temporal resolution	2 x 10 -3 s (RMS)

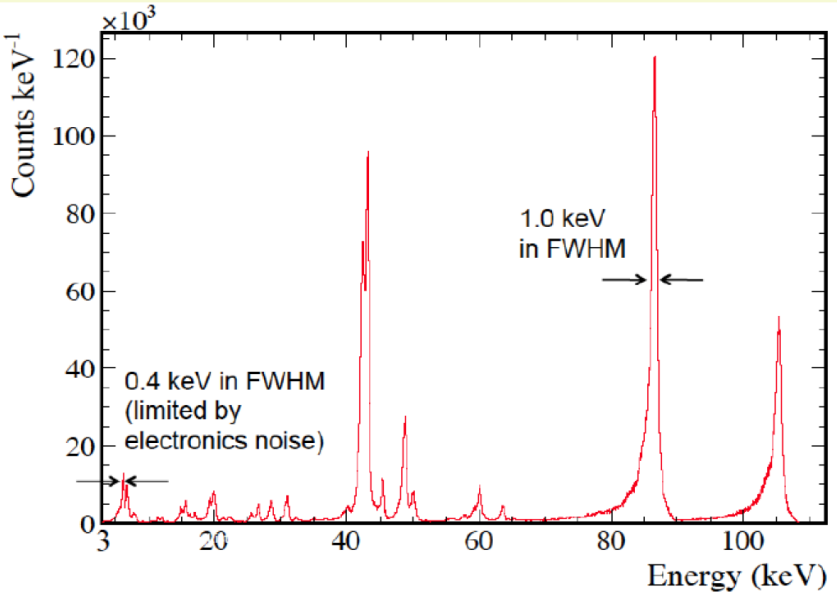

Inflight spectrum of the FPMB/DET0 detector irradiated with the onboard 155Eu radioactive source. The energy resolution (FWHM) is 0.4 keV below 50 keV and rises to 1.0 keV at 86 keV.

CHANDRA mission:

Energy resolution

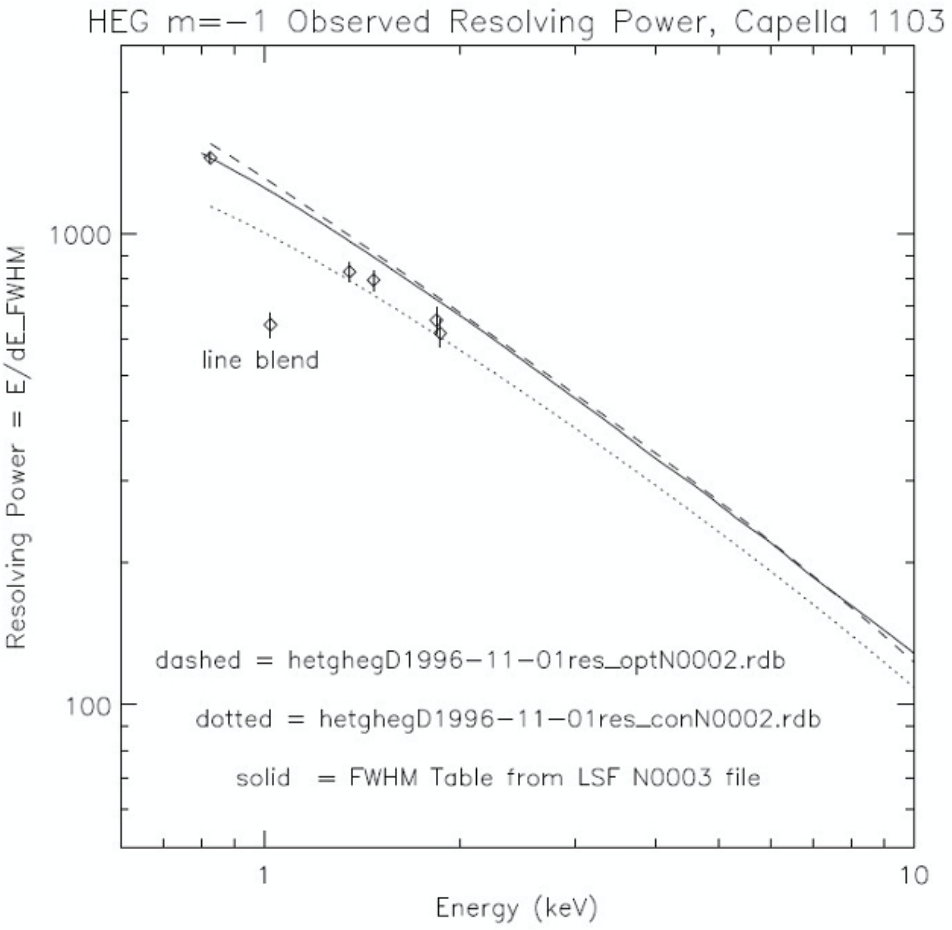

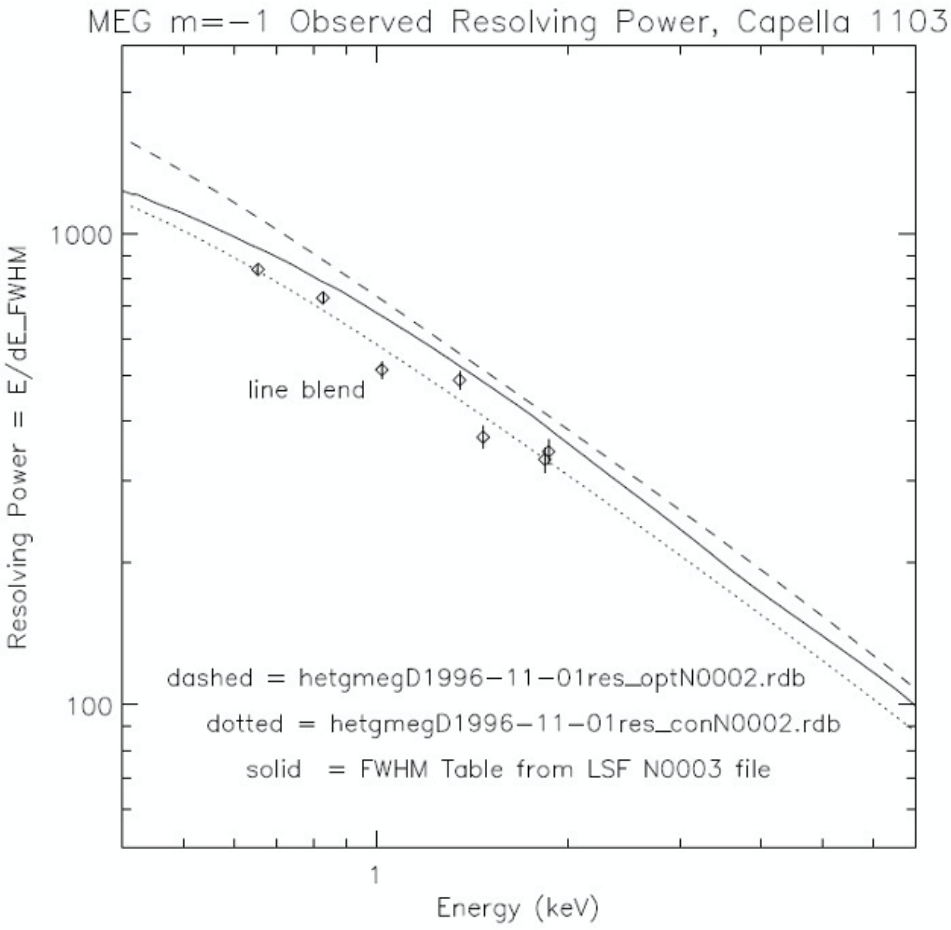

Effective area:

Chandra HEG

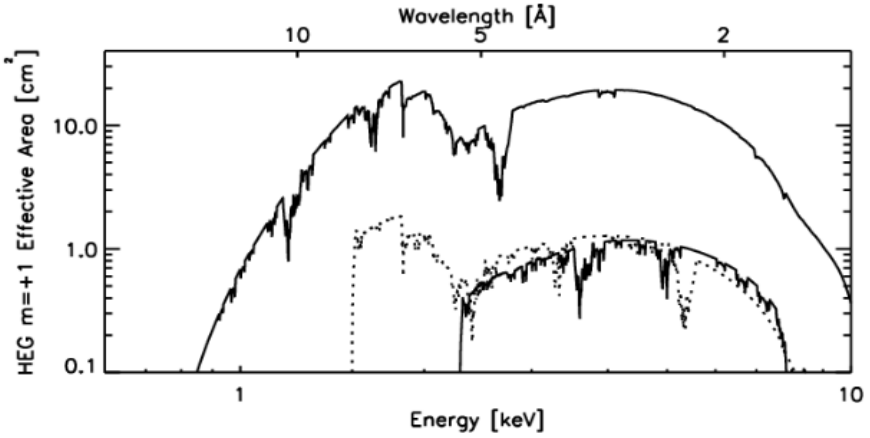

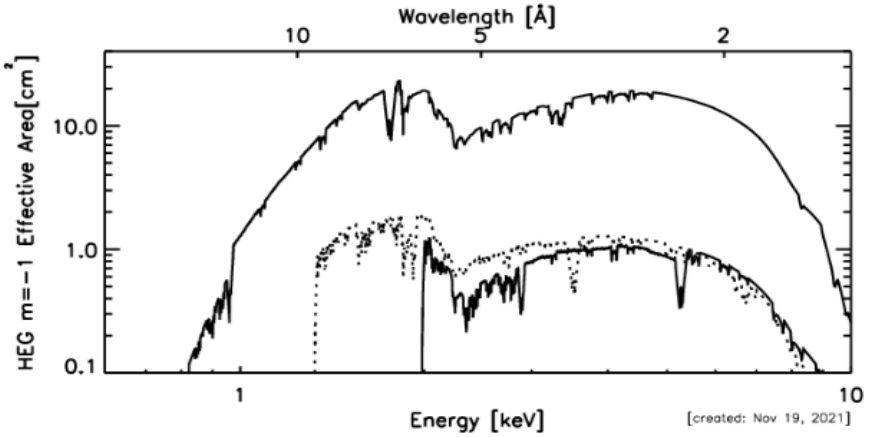

HITOMI

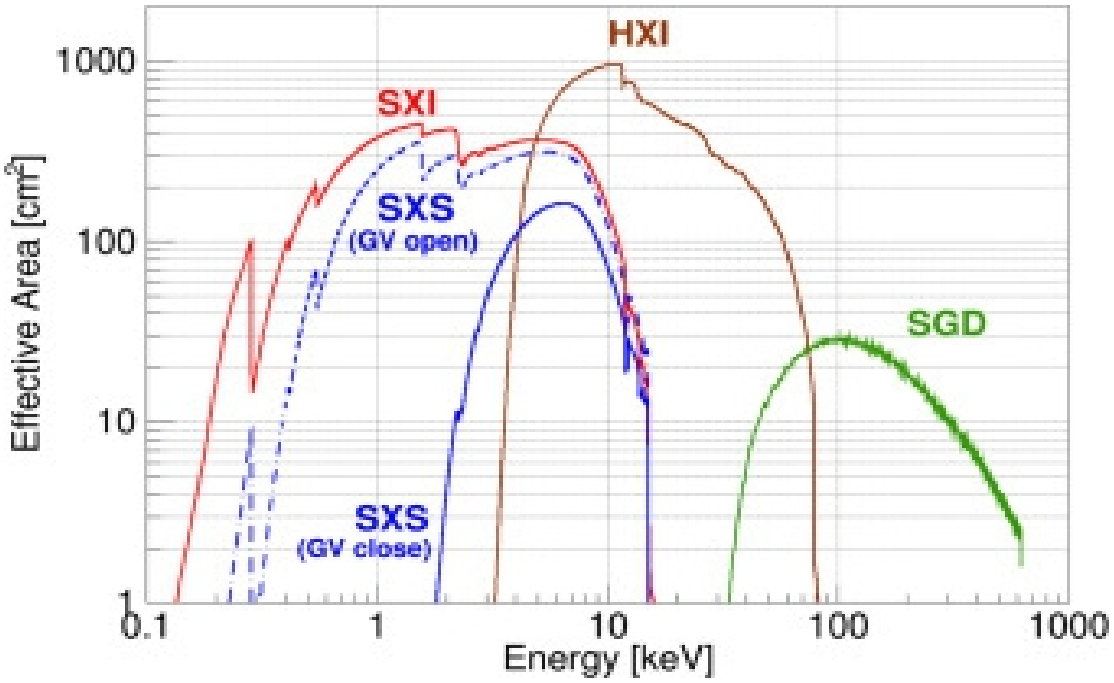

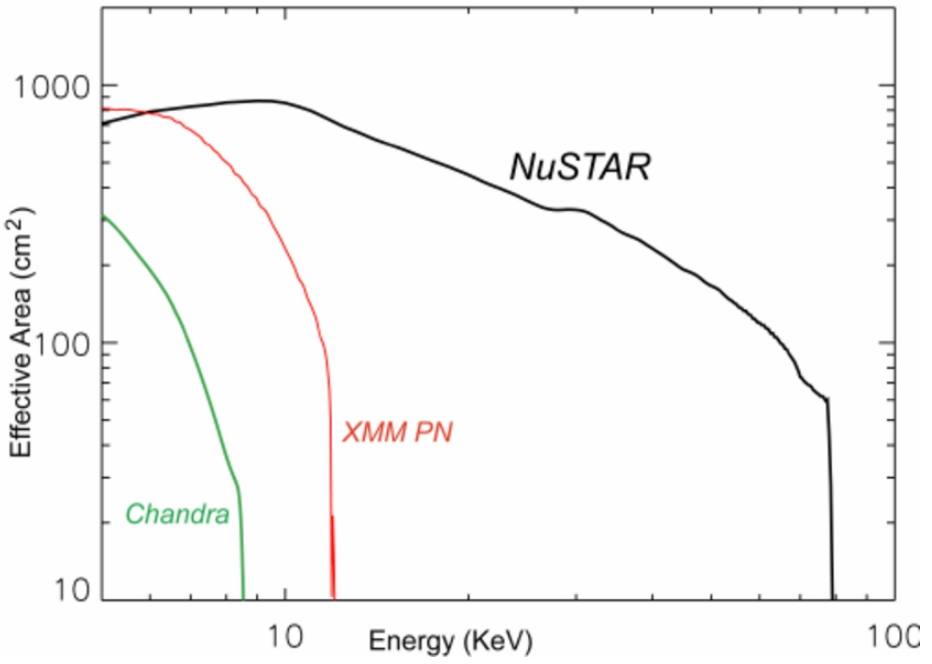

Effective area:

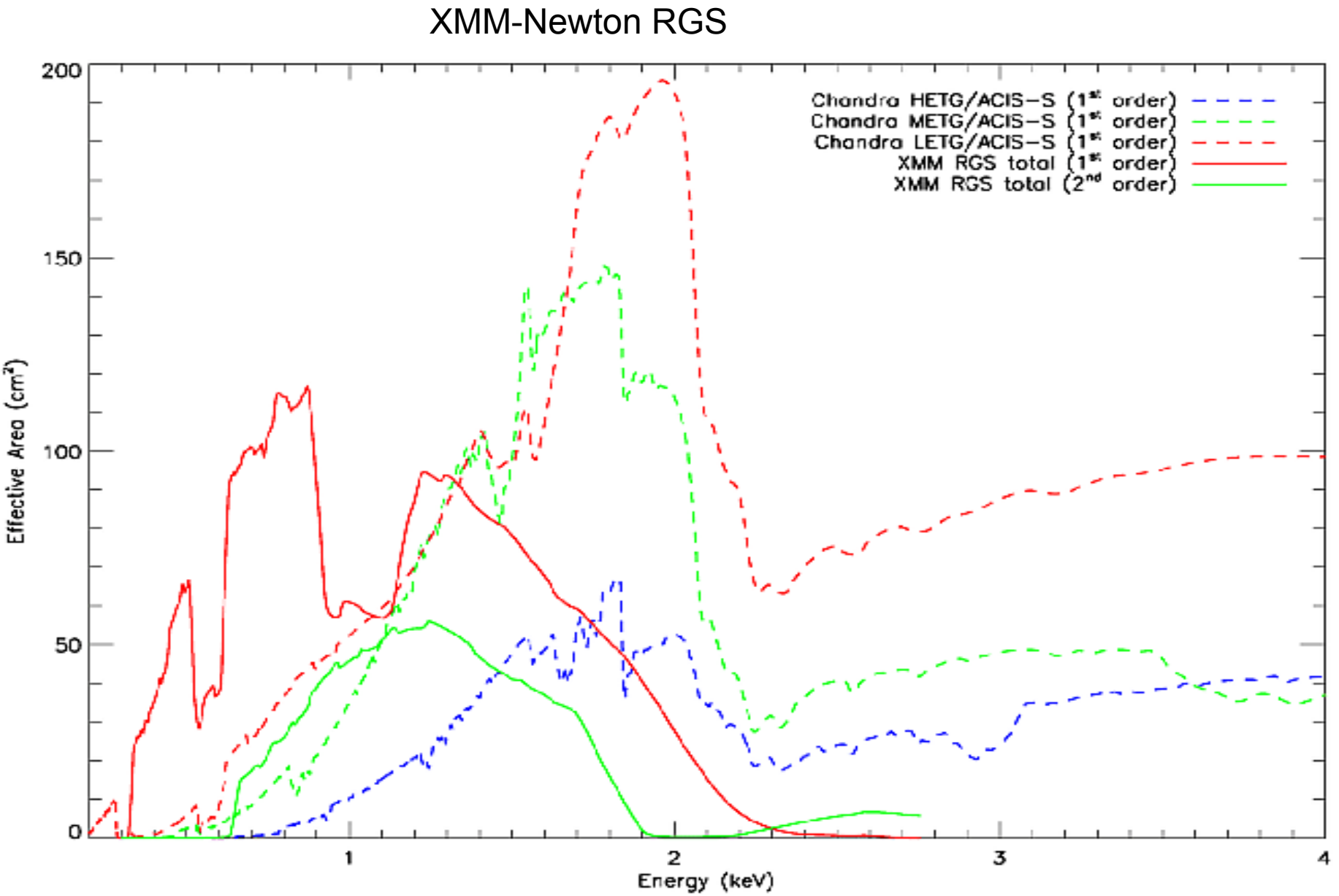

Effective area:

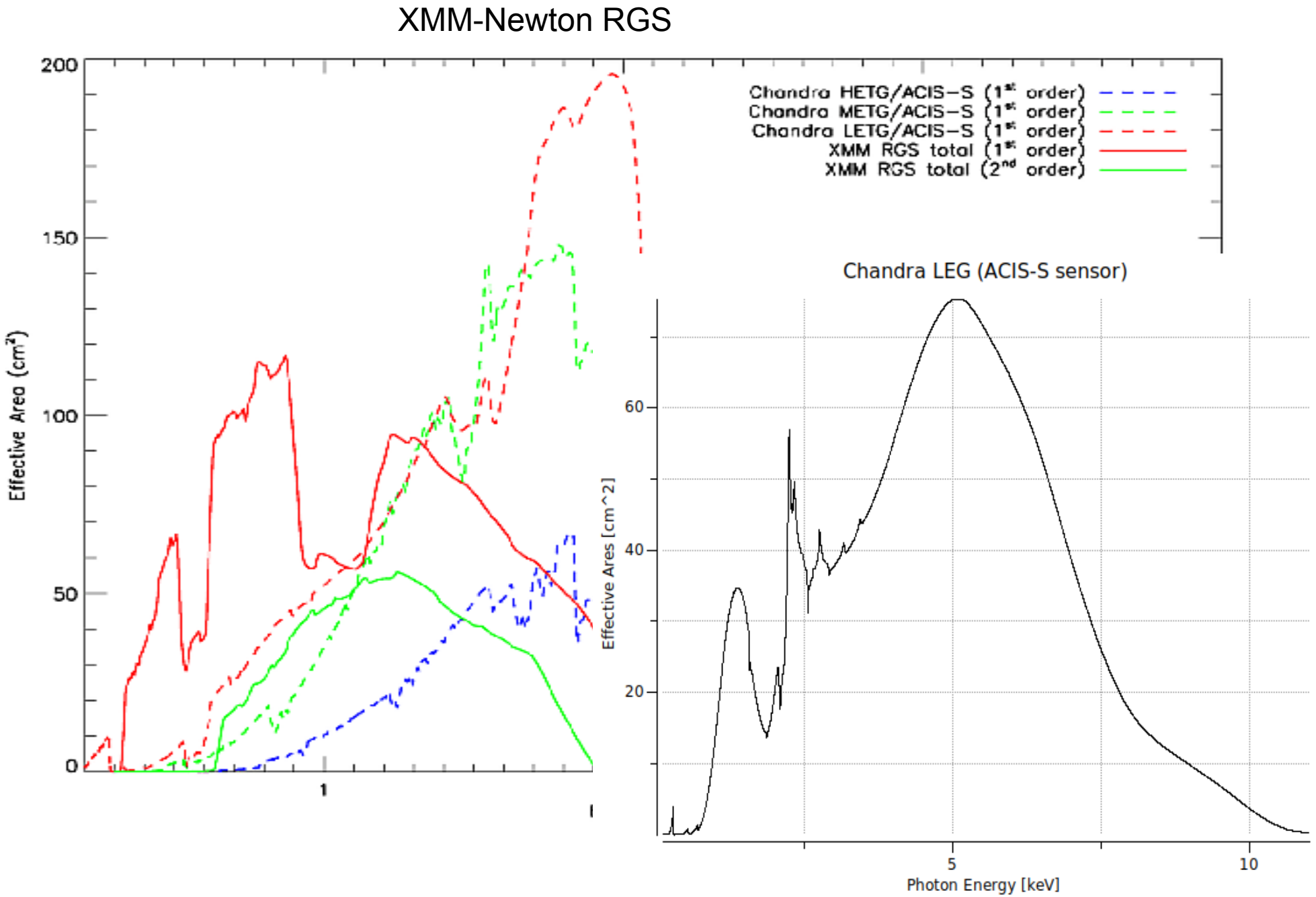

Effective area:

ASCA mission

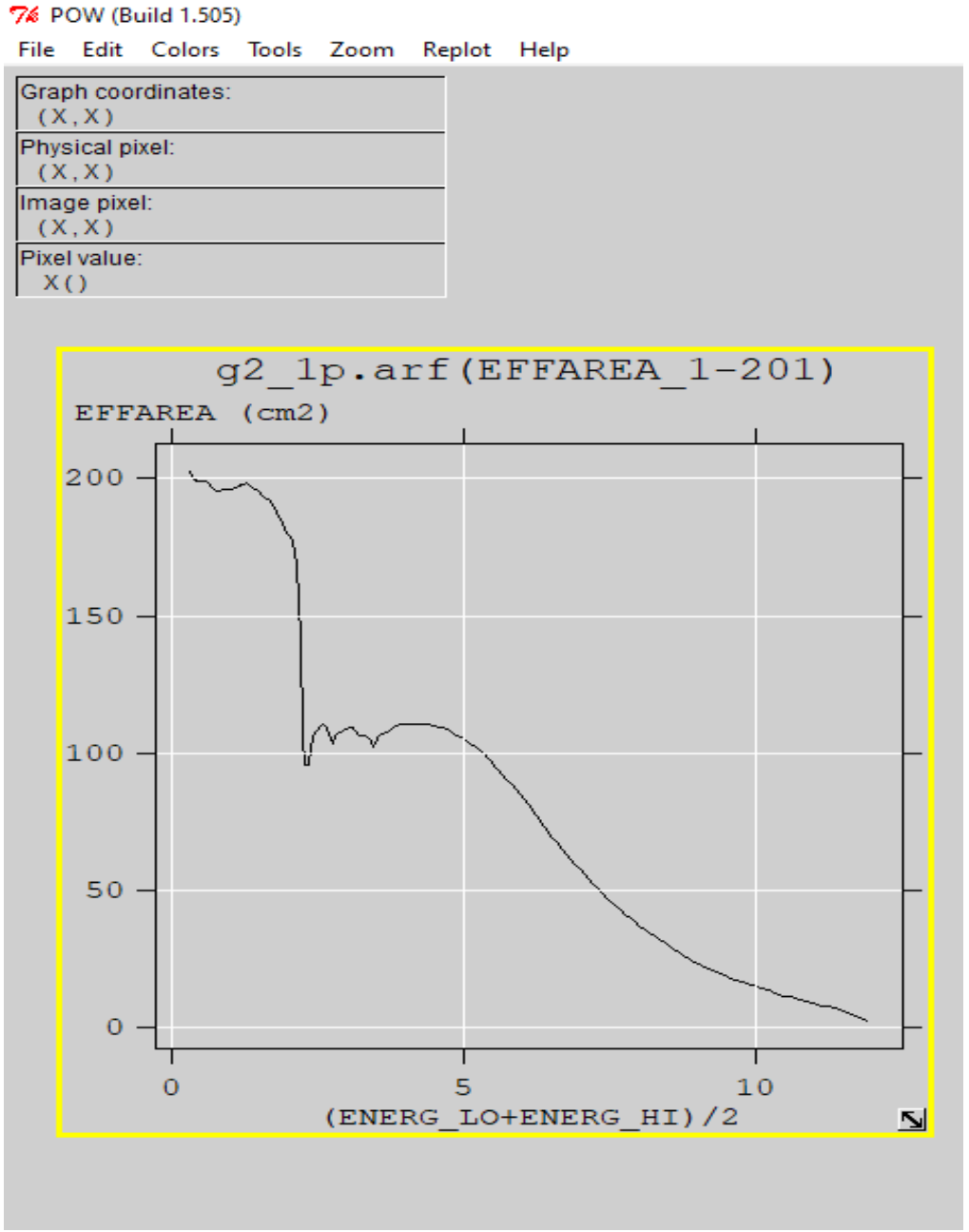

Effective area:

ASCA mission 1990-ties

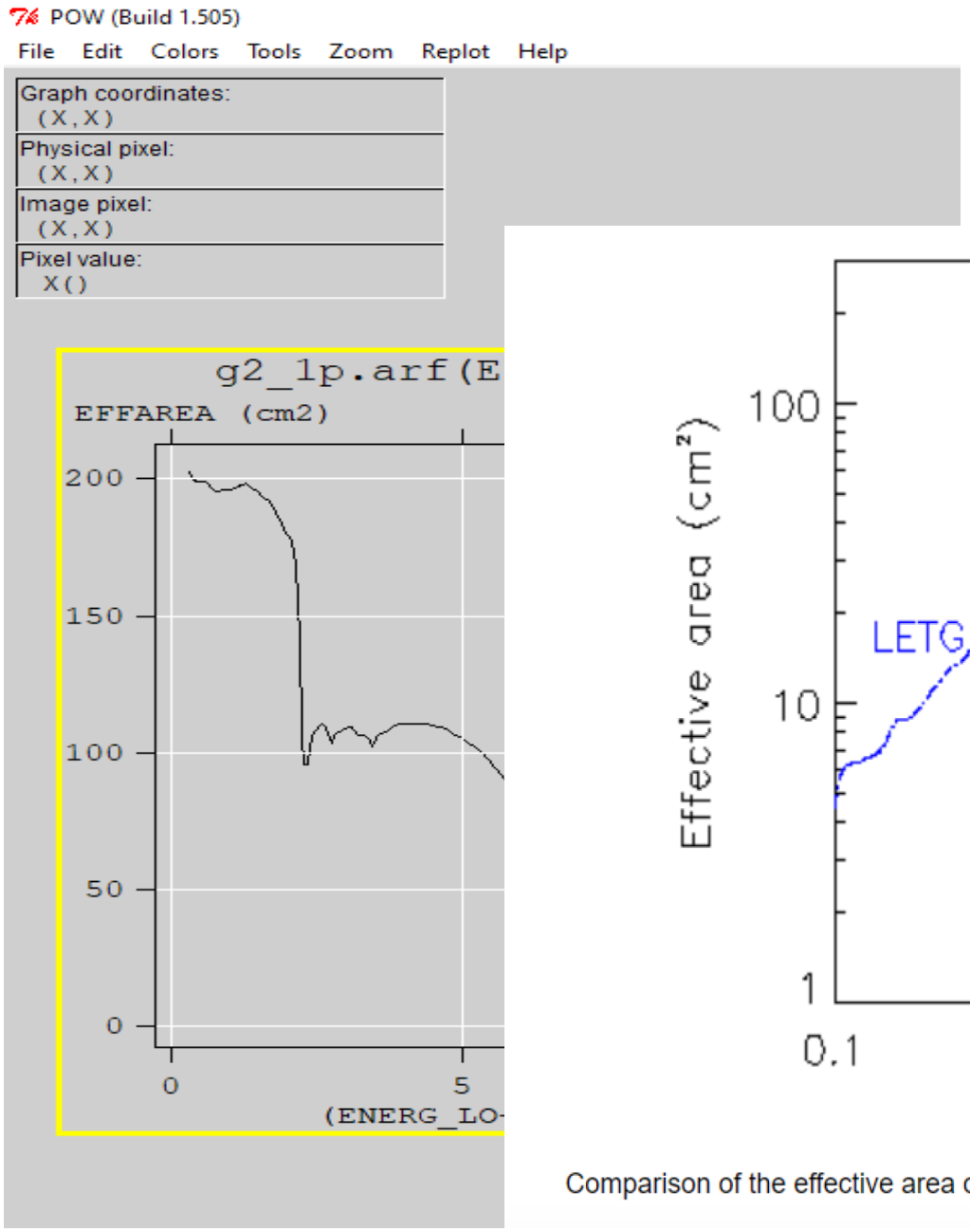

SUZAKU - 2005

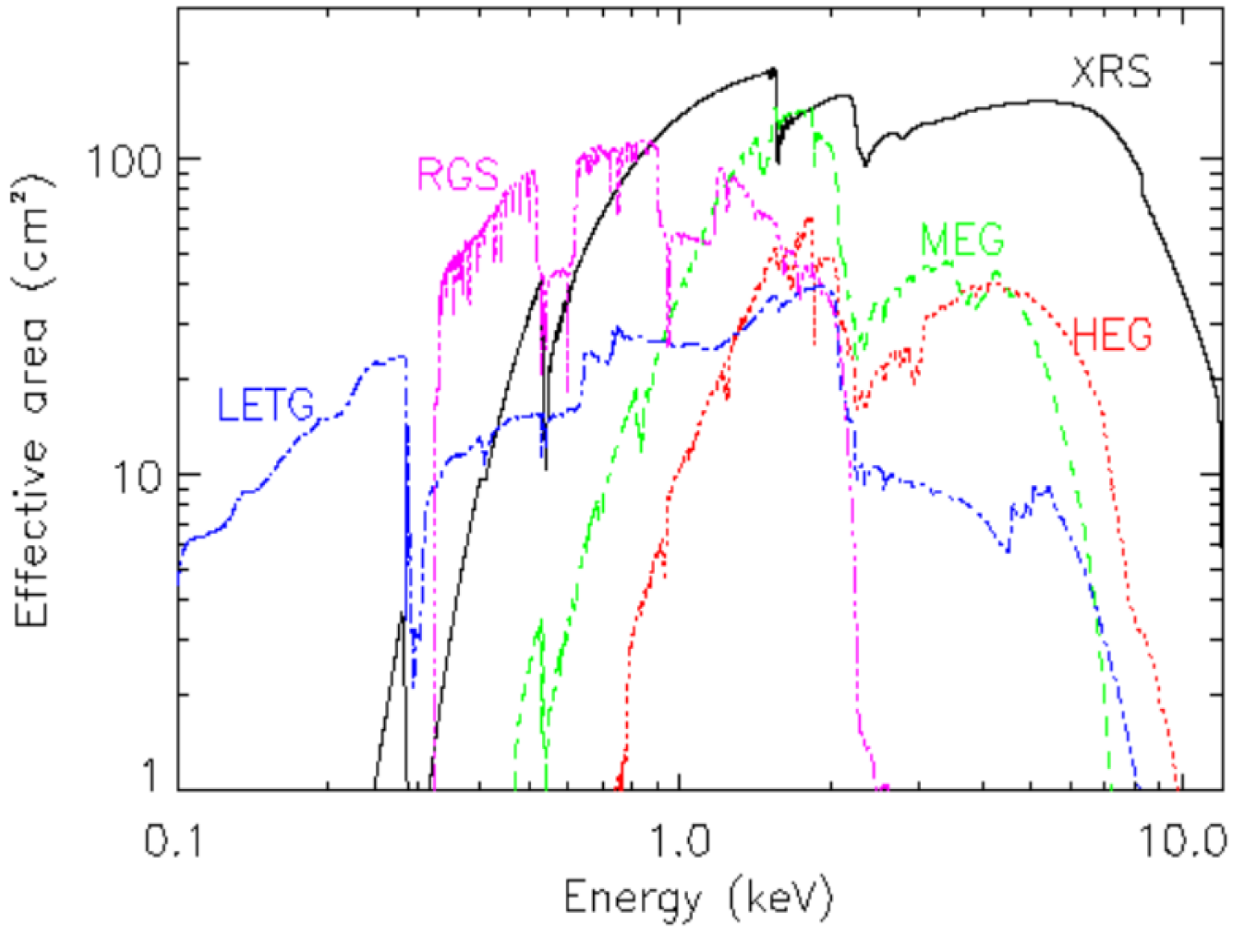

Comparison of the effective area of the XRS against the *XMM-Newton* RGSs and the *Chandra* grating instruments.

Spacial resolution

EINSTEIN mission:

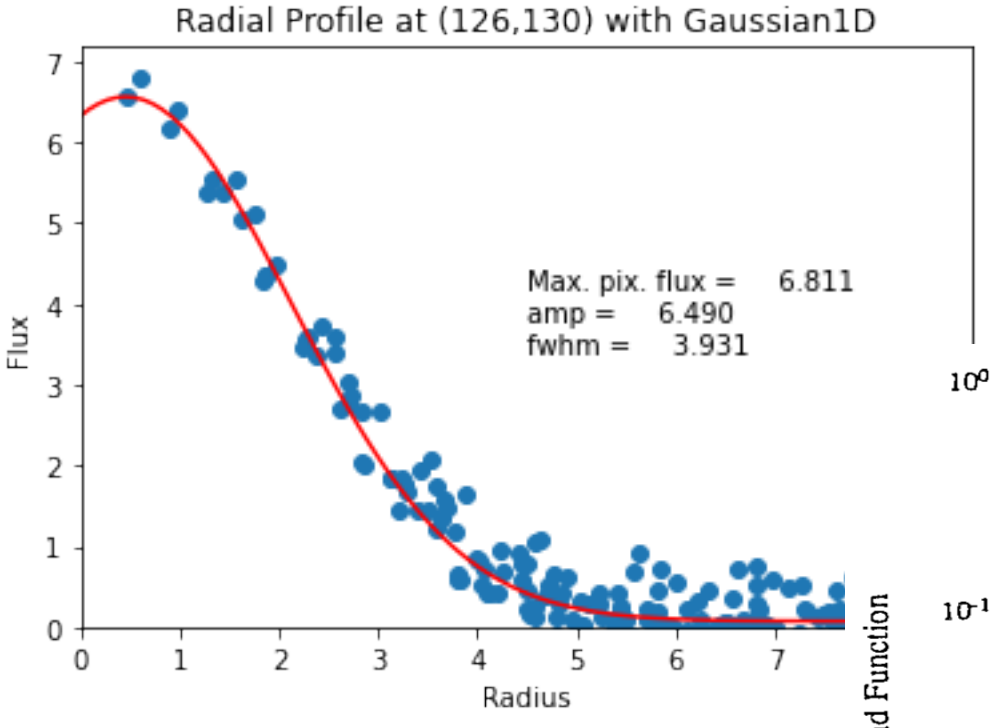

ASCA mission

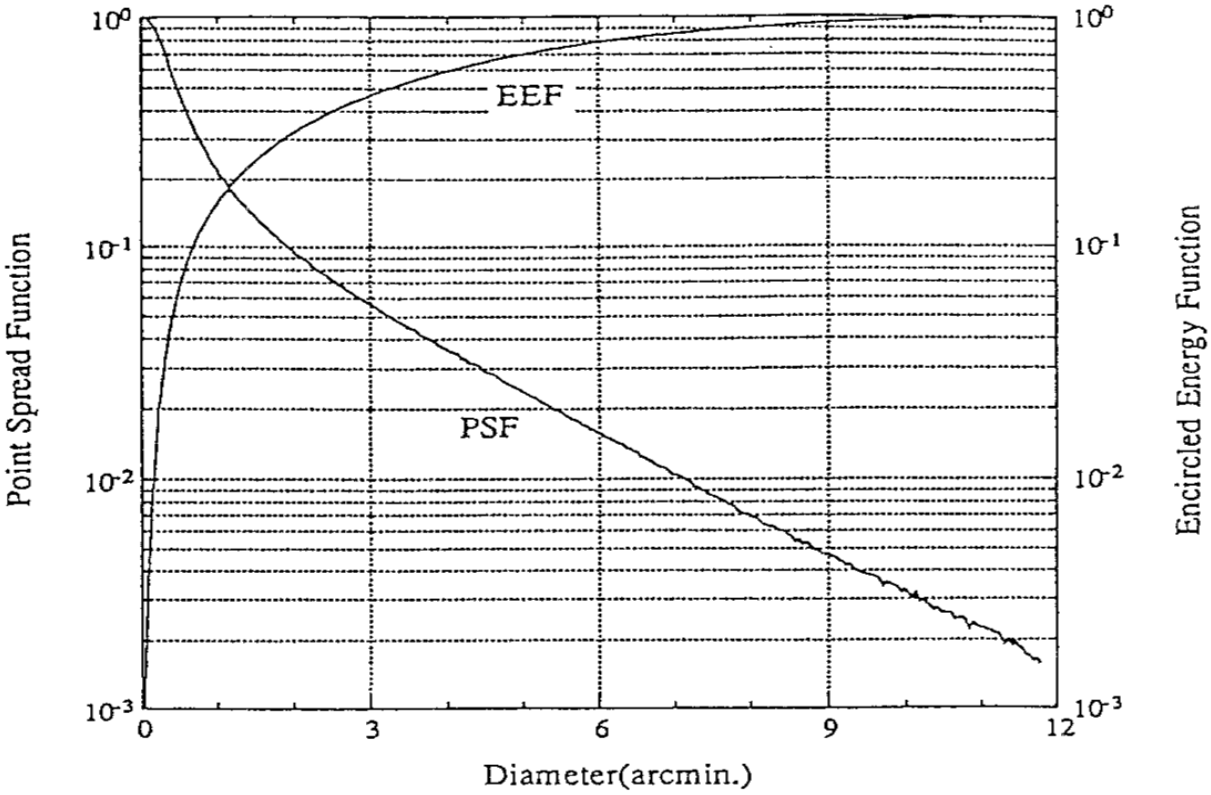

Figure taken from:

Tanaka, Y., Inoue, H. and Holt, S. S. 1994, "The X-ray Astronomy Satellite ASCA", Publ. Astron. Soc. Japan, 46, L37

Spacial resolution

Chandra mission:

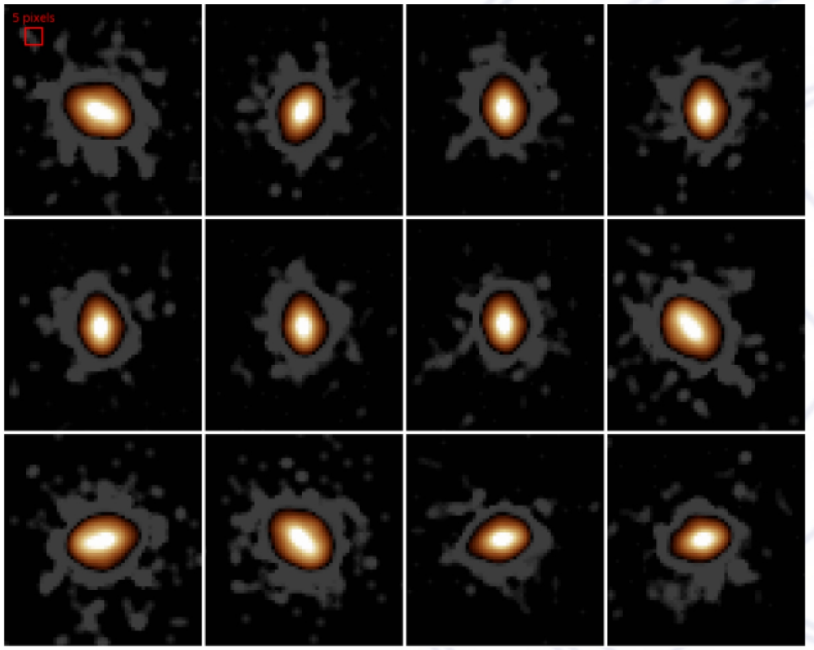

Figure 2: 12 examples of PSFs at 5' off-axis with various locations azimutha around the optical axis, with different detector configuration, and with differen

SUZAKU in detector coordinates

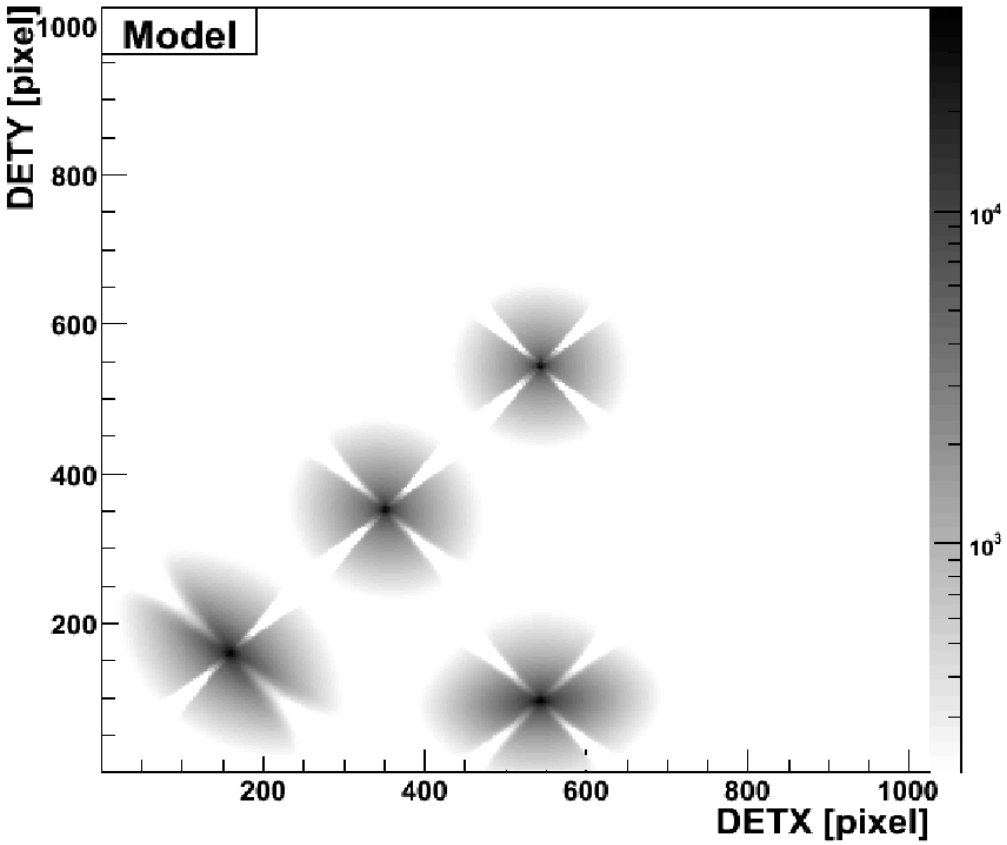

Resolution of telescope is related to point spread function.

Resolution of EXOSAT =18" (18 arcsec).

Summary after 5th and 6th lecture:

5th - Statistics, basic:

Poisson distribution:

- **discrete, independent events**
- **for small mean numbers**
- **asymmetric**
- **normalized to unity.**

Normal (Gaussian) distribution.:

- **differential probability**
- **normalized to unity**
- **symmetric around mean**
- **describes the random events for large m.**

Significance of measurement:

- **FWHM, "3 sigma" error**
- **standard deviation, variance**
- **propagation of errors.**

Background substraction:

- **signal-to-noise ratio**
- **low-B and high-B limits**
- **bright and faint sources.**

6th – Data reduction and calibration:

Event file:

- **sky position**
- **CCD pixel grade**
- **PHA informations**
- **GTI**
- **first BKGR rejection.**

Looking at the data:

- **bad pixels, pile-up**
- **selecting events of interest**

Extracting analysis products:

- **image – dithering**
- **spectrum – PHAS to PI**
- **light curve - CCD periodic readout.**

Calibration:

- **fundamental response equation**
- **PSF and EA response files for imaging**
- **ARF and RMF files for spectroscopy**
- **light curve - "dead time" corrections.**

Lecture 7: Data analysis

Any data analysis must begin with careful consideration of the physics underlying the emission before starting to progress through a series of software tools and scripts.

(Handbook for X-ray astronomy, 2011)

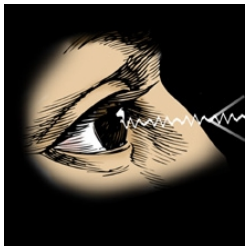

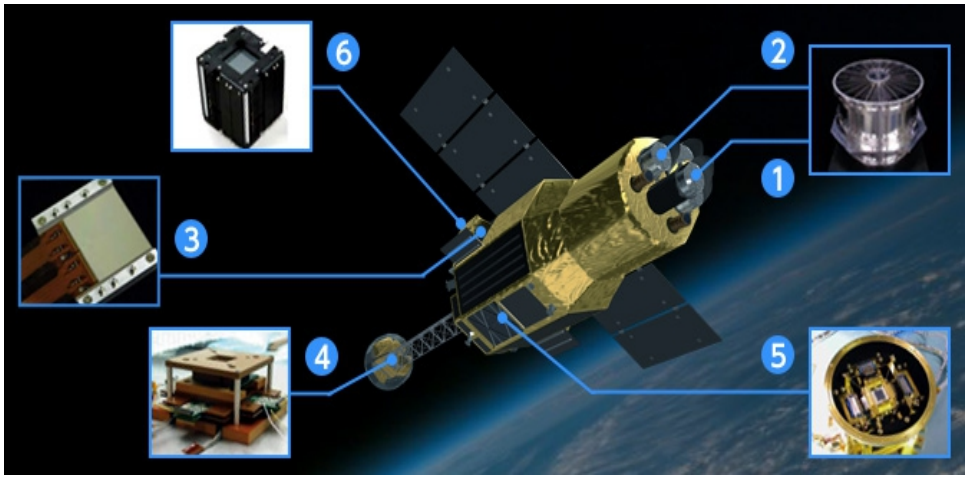

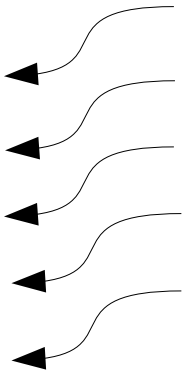

Observer Satellite, ASTRO-H Photons Source

1.Soft X-ray telescope
2.Hard X-ray telescope } **focusing X-ray**
3.Soft X-ray imager
4.Hard X-ray imager } **imaging CCD**
5.Soft X-ray spectrometer
6. Soft γ- ray detector

Archives, catalogs and software:

X-ray-astronomy observations are available on-line; the challenge is to find the right data.

CHANDRA - http:/cda.harvard.edu
NED - http://nedwww.ipac.caltech.edu
SIMBAD - http://simbad.u-strasbg.fr/simbad

Translate the name into a position

HEASARC – access to public data for all currently operating X-ray missions, and all major past missions.

HERA – http://heasarc.gsfc.nasa.gov/hera
is a software service provided by HEASARC, the analysis can be run on a server - /fv program or a web browser.

Archives, catalogs and software:

CXC – http://cxc.harvard.edu
responsible for CHANDRA – current archive,
WebChaSer – http://cda.harvard.edu/chaser
V&V – verification and validation report about data.
Chandra Fast Image – http://cda.harvard.edu/pop
quick look at the image.

SOC – http://xmm.esac.esa.int
XMM-Newton Science Operations Centre,
XSA – http://xmm.esac.esa.int/xsa
It uses "shopping basket" model for selecting observations.
BiRD – http://xmm.esac.esa.int/BiRD/index.html
Browsing interface for RGS Data – quick-look of spectra and images from gratings, combine multiple spectra, taking into account calibration, Gal. absorption and redshift.

Archives, catalogs and software:

Several other mirrors which may work better ..!!!

LEDAS – http://ledas-www.star.le.ac.uk Leicester University, UK
(Chandra, ASCA, ROSAT, Ginga)

DARTS – http://www.darts.isas.jaxa.jp at ISAS Japan
(Suzaku, ASCA, Ginga, Tenma)

ASDC – http:/www.asdc.asi.it in Italy
(Chandra, XMM-Newton, Swift, BeppoSax, ROSAT)

VO - http://heasarc.gsfc.nasa.gov/cgi-bin/vo/datascope/init.pl
DataScope makes the data available to VO tools.

Archives, catalogs and software:

RASS – http://skyview.gsfc.nasa.gov 0.1-2.5 keV band,
ROSAT All-Sky Survay: SkyView
RASSfsc, RASS2mass, RASSdsstar, RASSebcs.

Chandra Source Catalog:
ChaMP – in the galactic plane,
Xassist – automated processing of all public Chandra obs.
Brera Multi-scale Wavelet Chandra Catalog –
wavelet source-finding algorithm on all ACIS-I observations.
Chandra Deep Field North – CDFN
Chandra Deep Field South – CDFS
ANCHORS – Chandra star-formation observations.

XCS – entire XMM-Newton public archive.
RXTE All-Sky Monitor (ASM) – 2-10 keV

Archives, catalogs and software:

Two basic classes of software tools:

- mission-dependent
- mission-independent

Packages:

HEAsoft – referred to as FTOOLS, from the HEASARC,
CIAO – produced by the CXC,
SAS – produced by the XMM-Newton SOC,

Using the IDL system:

TARA – http://www.astro.psu.edu/xray/docs/TARA
vizualization and analysis including ACIS Extract program.

Archives, catalogs and software:

Software to manipulate event files:

xselect – the HEA soft program to filter event files,
extractor

dmcopy – CIAO filtering tools
dmextract

evselect – SAS filtering tool
xmmselect – the same but GUI version (Graphical User Interface).

Archives, catalogs and software:

Imaging-analysis software:

DS9 – from SAO (Smithsonian Astrophysical Observatory)

fv – FITS viewer, can create image from any two columns in the event file.

Spectral-analysis software:

XSPEC – from HEASARC

Sherpa – from CIAO

ISIS – for high-resolution spectroscopy MIT Chandra HETG group.

SPEC – http:/www.sron.nl/divitions/hea/spex
from SRON in Utrecht, collisional plasma, and high resolution spectroscopy

Timing-analysis software:

Xronos – from HEAsoft

SITAR – has a set of functions which can run in ISIS

Archives, catalogs and software:

Calibration data:

CALDB – calibration database of HEASARC

CCF – Current Calibration File, the collection of all XMM-Newton calibration files ever made public and is continuously updated.

cifbuild – the index file tool, created by the SAS, to identify which calibration elements are required.

DATA ANALYSIS:

PSPC had typically $R \equiv E/\Delta E \sim 1-10$

CCDs tend to have higher backgrounds, small pixels, and substantially better resolution:

$$R \equiv E/\Delta E \sim 10-50$$

Spectral fitting:

$$C(PI) = T \int RMF(PI, E) \cdot ARF(E) \cdot S(E) \cdot dE$$

DATA ANALYSIS:

PSPC had typically $R \equiv E/\Delta E \sim 1-10$

CCDs tend to have higher backgrounds, small pixels, and substantially better resolution:

$$R \equiv E/\Delta E \sim 10-50$$

Spectral fitting:

$$C(PI) = T \int RMF(PI, E) \cdot ARF(E) \cdot S(E) \cdot dE$$

$$C(PI) \approx T \sum_j R_{ij} A_j S_j$$

DATA ANALYSIS:

Spectral fitting: $$C(PI) \approx T \sum_j R_{ij} A_j S_j$$

C(PI) – observed counts in detector channel PI,
T – time of observation in seconds,
$\mathbf{S_j}$ – the source flux in photons/cm^2/s/keV,
$\mathbf{A_j}$ = ARF(E) is energy-dependent effective area in cm^2
$\mathbf{R_{ij}}$ = RMF(PI,E) is the unitless response matrix,
probability of an incoming photon of energy E being observed in channel PI.

Important is to use energy bins narrow compared to the detector resolution. Each mission provides those files for every telescope/detector combination.

DATA ANALYSIS:

Spectral fitting: $$C(PI) \approx T \sum_j R_{ij} A_j S_j$$

FREDHOLM integral equation of the first kind, resists easy solution for S(E) by direct inversion of R_{ij}.

But due to: - statistical and systematic errors of C(PI),
- calibration uncertainties of R_{ij} and A_j,
- extreme non-linearity of S_j arising from emission and absorption features in the spectrum,

DATA ANALYSIS:

Spectral fitting: $$C(PI) \approx T \sum_j R_{ij} A_j S_j$$

FREDHOLM integral equation of the first kind, resists easy solution for S(E) by direct inversion of R_{ij}.

But due to: - statistical and systematic errors of C(PI),
- calibration uncertainties of R_{ij} and A_j,
- extreme non-linearity of S_j arising from emission and absorption features in the spectrum,

usually leads to results that are dominated by noise.

The normal approach to to X-ray spectral analysis is to use **FORWARD FITTING.**

DATA ANALYSIS:

FORWARD FITTING: $$C(PI) \approx T \sum_j R_{ij} A_j S_j$$

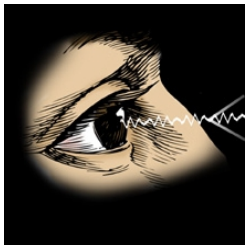

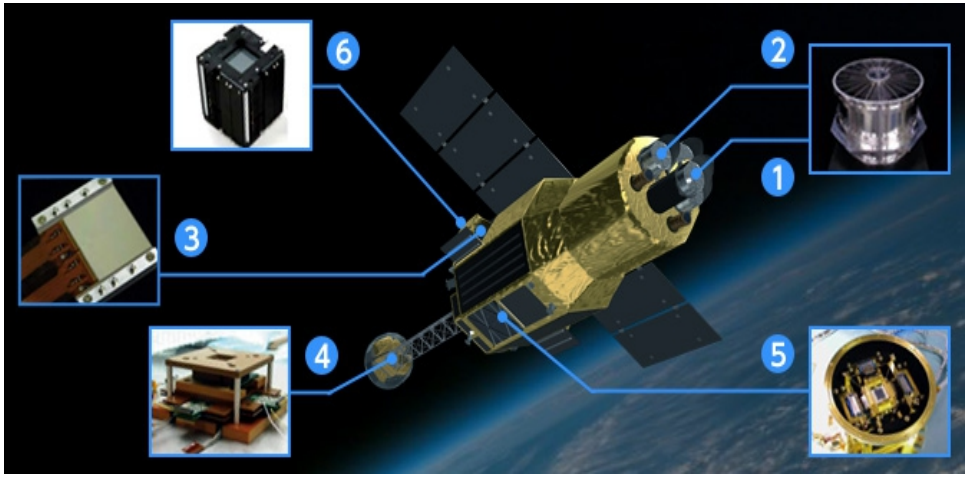

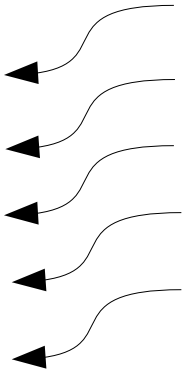

$C(PI)$ $R_{ij} A_j$ S_j

DATA ANALYSIS:

FORWARD FITTING: $C(PI) \approx T \sum_j R_{ij} A_j S_j$

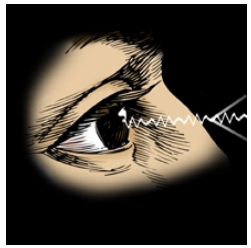

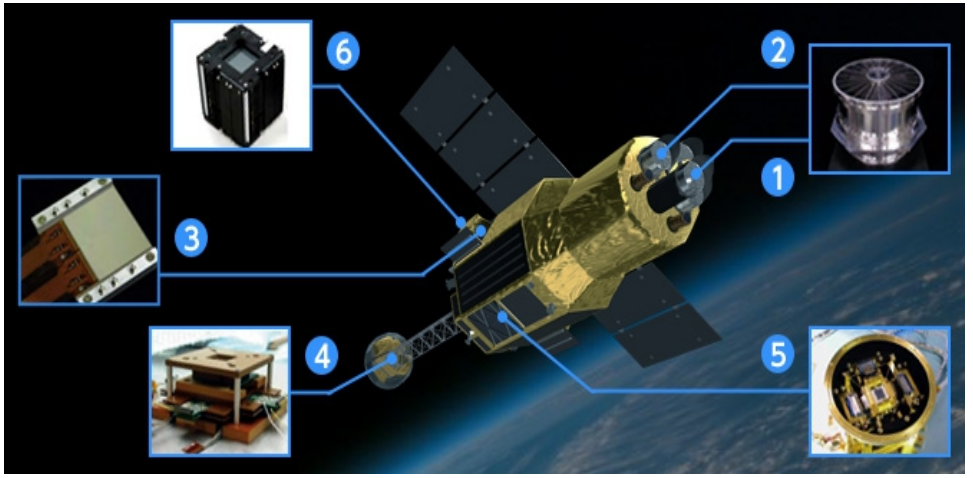

$C(PI)$ → unfolded spectrum → S_j

↑ fitting

convolution with response

theoretical model:

$B(PI)$ ← $R_{ij} A_j \times M_j$ ← M_j

DATA ANALYSIS:

Models – theory.... third part of the lecture.

Essentially, all models are wrong, but some are useful.
(Box & Draper 1987)

The aim of spectral fitting is to gain physical insight and that all models are likely to be oversimplified in some way.
(Handbook of X-ray Astronomy 2011)

Two basic types of models:

- additive - the emission component, such as a BB or spectral lines,
- multiplicative – component which modifies the spectrum such as an edge or absorption line.

But also convolution components, pile-up model, mixing models for multiple spectra.

DATA ANALYSIS:

Spectral-analysis software:

XSPEC
Sherpa
ISIS
SPEC

Table 5.1 *Physical processes and XSPEC models*

Physical process	XSPEC models[1]
Equilibium collisional plasma	(b)(v)apec, (z)(v)bremss, c6(p)(vm|me)kl, ce(vm|me)kl, equil, (v)meka(l), (v)raymond, smaug
Non-equilibrium collisional plasma	(v)(g)nei, (v)(n)pshock, (v)sedov
Photoionized plasma	absori, redge, swind1, xion, zxipcf
Power-law	bkn2pow, bknpower, cutoffpl, pegpwrlw, plcabs, (z)powerlaw
Blackbody	(z)bbody, bbodyrad
Emission line	(z)gaussian, diskline, kerrdisk, laor(2), lorentz
Compton scattering	bmc, cabs, comp(LS|PS|ST|TT|bb), nthComp, simpl
Accretion disk	disk(bb|ir|m|o|pbb|pn), ezdiskbb, grad, hrefl, kdblur(2), kerr(bb|d|conv), rdblur, sirf, xion
Reflection	(b|p)exr(a|i)v, (i)reflect, refsch
Neutron-star atmosphere	nsa(grav|atmos), nsmax
Cooling flow	(mk)(vm)cflow
Gamma-ray burst	grbm
Pair plasma	nteea
Positronium continuum	posm
Synchrotron	srcut, sresc
Photoelectric absorption	absori, edge, partcov, pcfabs, (v)phabs, pwab, smedge, swind1, tb(var)abs, tbgrain, varabs, wndabs, zvfeabs, zxipcf
Cyclotron absorption	cyclabs
Dust scattering	dust
Reddening	redden, uvred, zdust, zsmdust

Practical considerations:

The more complicated the model and
the more highly correlated the parameters then the more likely that the algorithm will not find the true minimum.

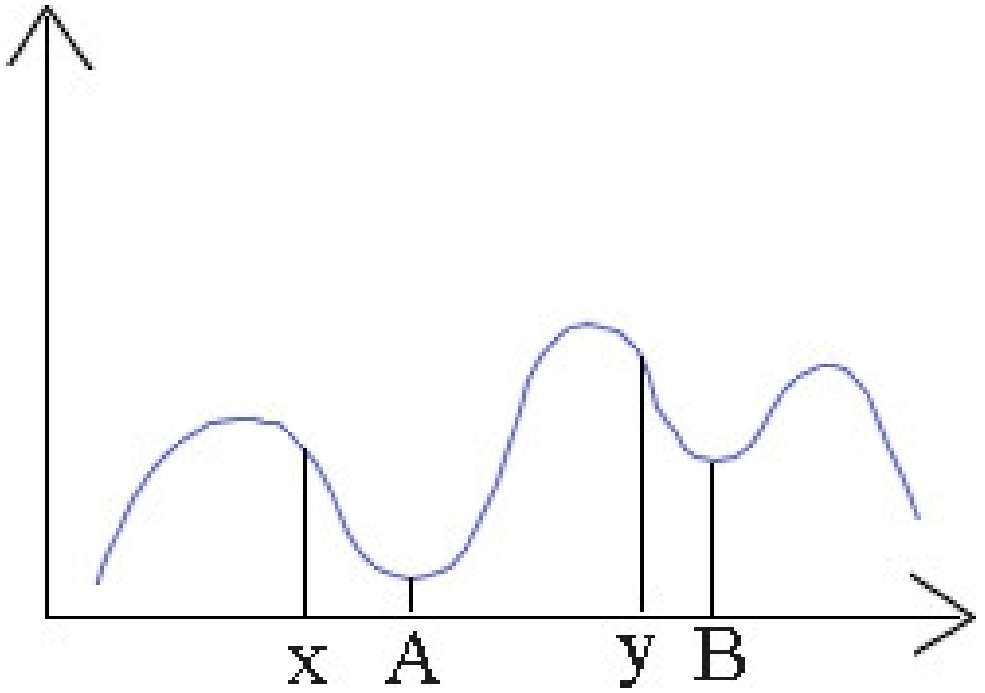

Local minimization
– at point B,

Global minimization
– at point A,

Depends how do we start.

Solution: to estimate the confidence error - **STATISTICS.**

Dealing with background:

For imaging detectors it is usual to extract a bkgr from a source-free region.
For non-imaging detectors a bkgr spectrum is calculated using methods developed by the instrument team.
The best method (Broos + 2010) is to fit simultaneously the bkgr and source spectra with models:

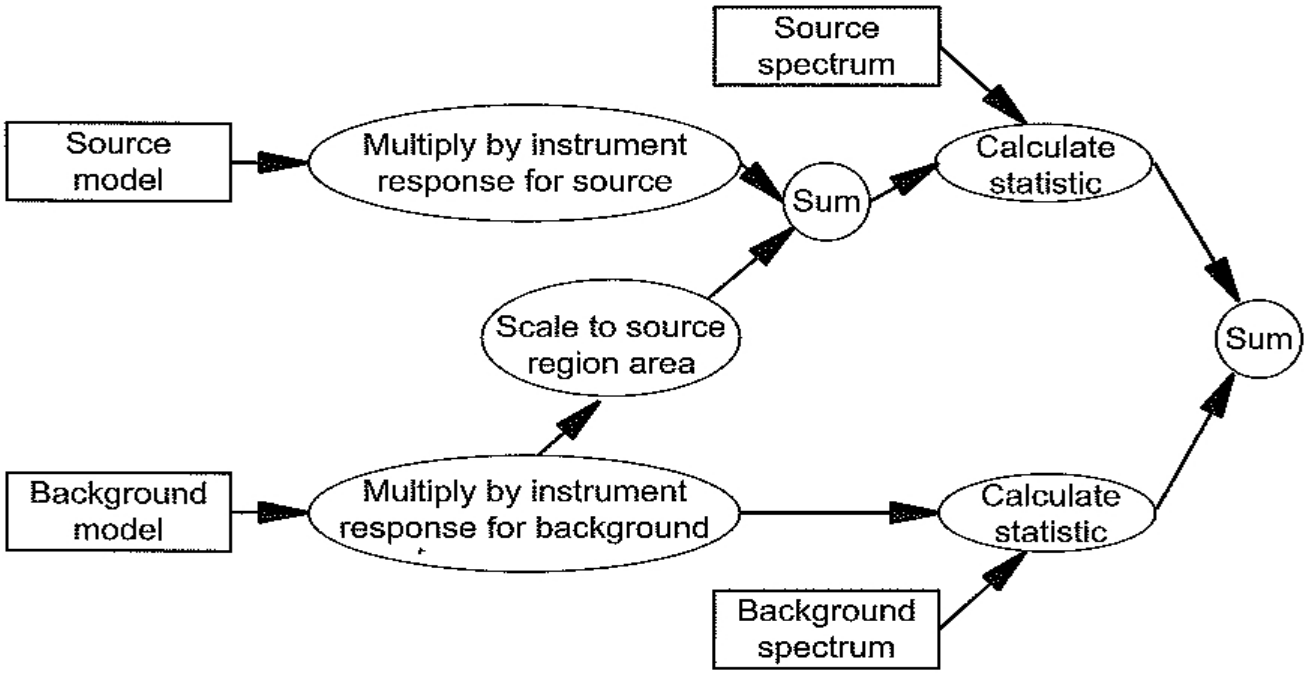

Fig. 5.7 Flowchart (after Broos *et al.*, 2010) showing the procedure for simultaneously fitting source and background

Dealing with background:

If the bkgr model is not available, and the data have Gaussian errors, S^2 statistic can be used. The difference of two Gaussian distributions is also Gaussian..... (Siemiginowska+2011 see: Krivonos + 2010 ?)

If the data have Poisson errors the problem is difficult, since the difference of two Poisson distributions does not have a simply analytic for.

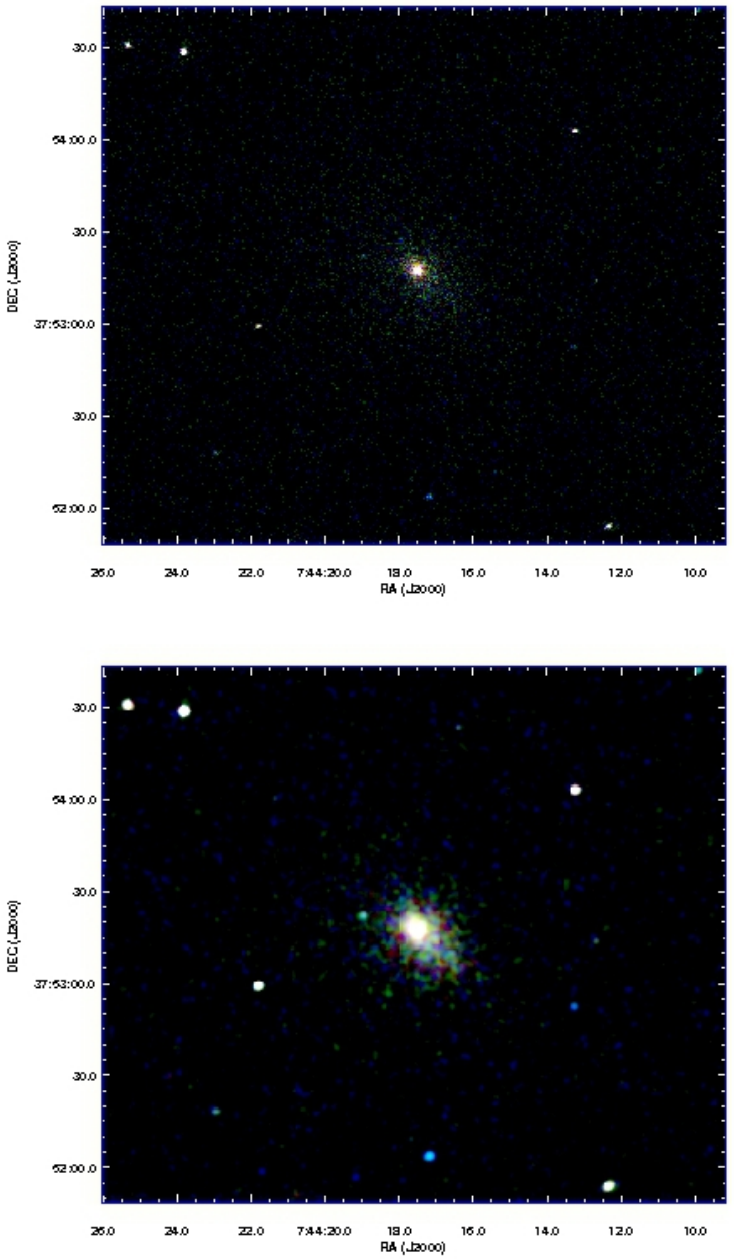

FIG. 1. RGB color *Chandra* ACIS-S images of the 3C186 X-ray cluster. The four individual observations have been merged into one image. Colors represent different energies: red:0.3-1.5 keV, green:1.5-2.5 keV and blue:2.5-7 keV. Top: Images binned to ACIS-S pixels with the standard size of 1 pixel=0.492 arcsec. Bottom: The image has been smoothed by a Gaussian function of $\sigma = 2.46''$.

Source characterization:

Is the source a point-like or extended?
The easies approach is to calculate the radial profile of the source and compare this to the mirror PSF, Siemiginowska + 2003

If the source is relatively faint, the PSF is elliptical.
More advanced approach, to use mirror PSF as the “response” of the telescope and convolve it with a δ function or Gaussian.
If the δ function fits the image then the source is point-like or unresolved by the telescope.

DATA ANALYSIS:

Imaging analysis

The goals are similar to those in other wavebands:

- identification of sources down to some limit,
- discrimination between extended and point sources,
- identification of structure in extended sources,
- variability in different spectral bands.

X-ray images:

1) low count rates,
   < 10 counts in total,
2) large changes of PSF
   over the detector FOV.

HPD – half-power diameter
for Suzaku PSF is ≈ 120 arcsec.

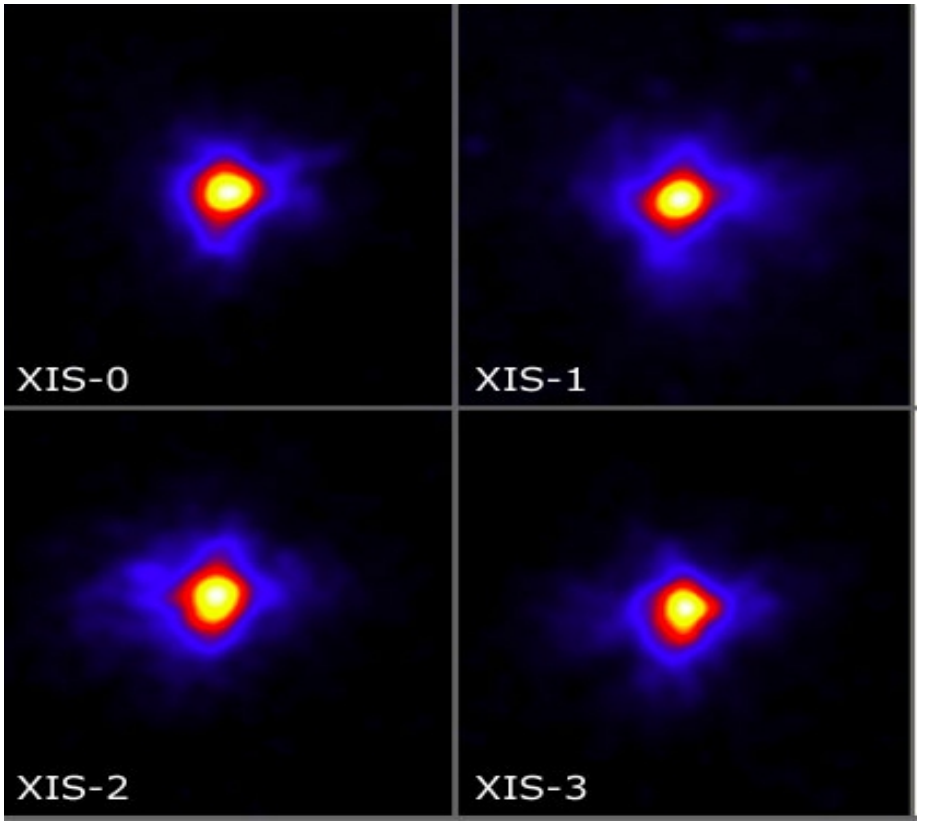

Source detection:

celldetect – CIAO data analysis software to determine source and bkgr fluxes by convolving 2D image data with predefined shaped filters.
The filter size depends on PSF.

The original sliding-cell algorithm uses a box-shaped filter with larger box for bkgr than the source.

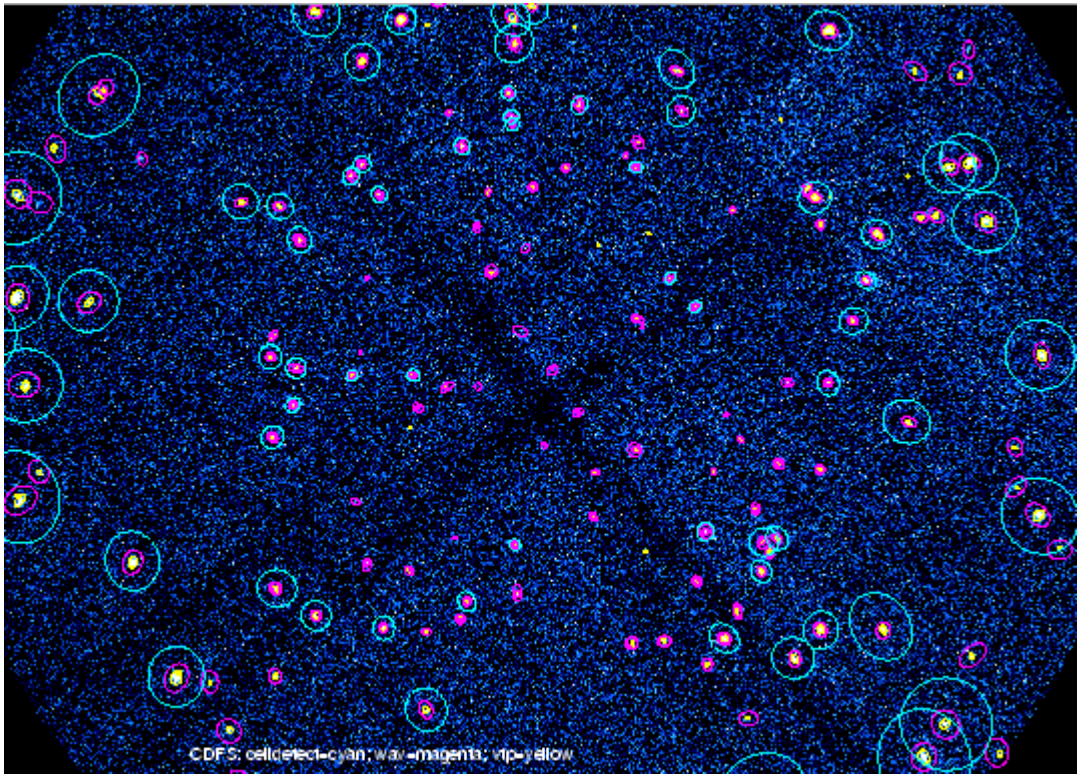

Problem with crowded sources and at the detector edge.

CDFS with ACIS-S, only data within 8' of the center were accepted

Source detection:

Wavelet basis functions e.g. the Mexican Hat.

pwxdetect – the code developed in Palermo, allows to for multi-scale analysis of mexican-hat wavelet convolved images.

Pillitteri + 2010 Wavelets can better match the PSF shape this method nicely works in crowded fields. Asymmetric sources are NOT resolved.

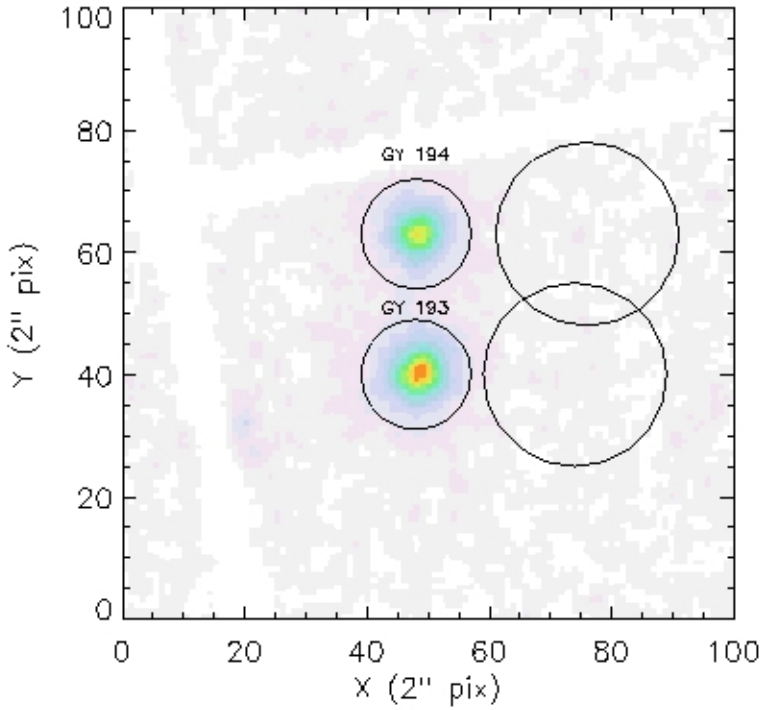

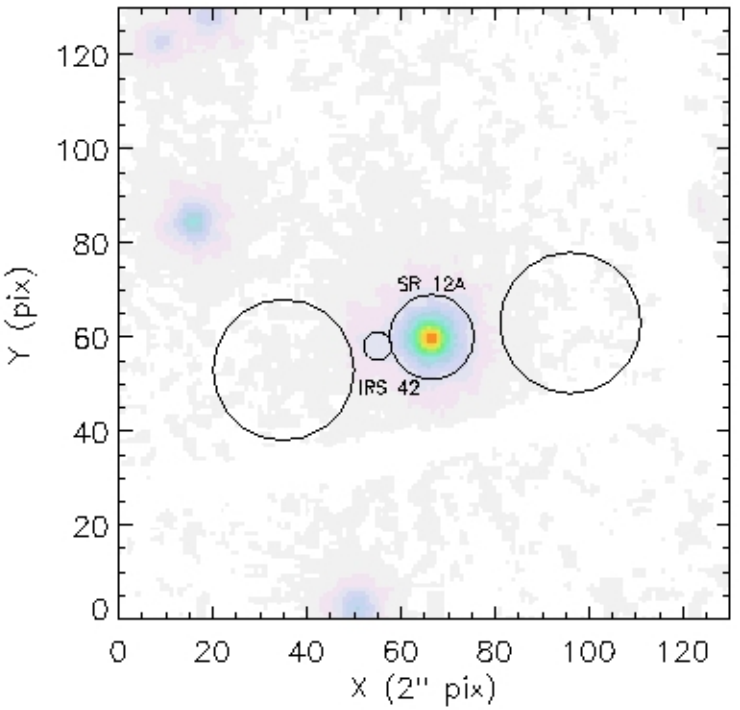

Source detection:

Voronoi-Tesselation-Percolation algorithm, Ebeling + 2001

vtpdetect – in CIAO works directly with X-ray events, so the data are not binned and the precise position of each photon is used. Assumes Poisson distribution for bkgr.

The algorithm detects both point sources and diffuse emission irrespective of the shape of that emission and its geometry.
It is also sensitive to low surface-brightness emission and it is more efficient than the previous methods in detecting sources.

Masimum-likelihood method, Cruddace + 1988

emldetect – in SAS, likelihood function for the entire image for all possible sources given the bkgr.

However, they require efficient optimization algorithms.

Chandra Ray Tracer CHART,
two point sources separated by 2"

Siemiginowska + 2003

X-ray jet discovery in the distant quasar z=4.3

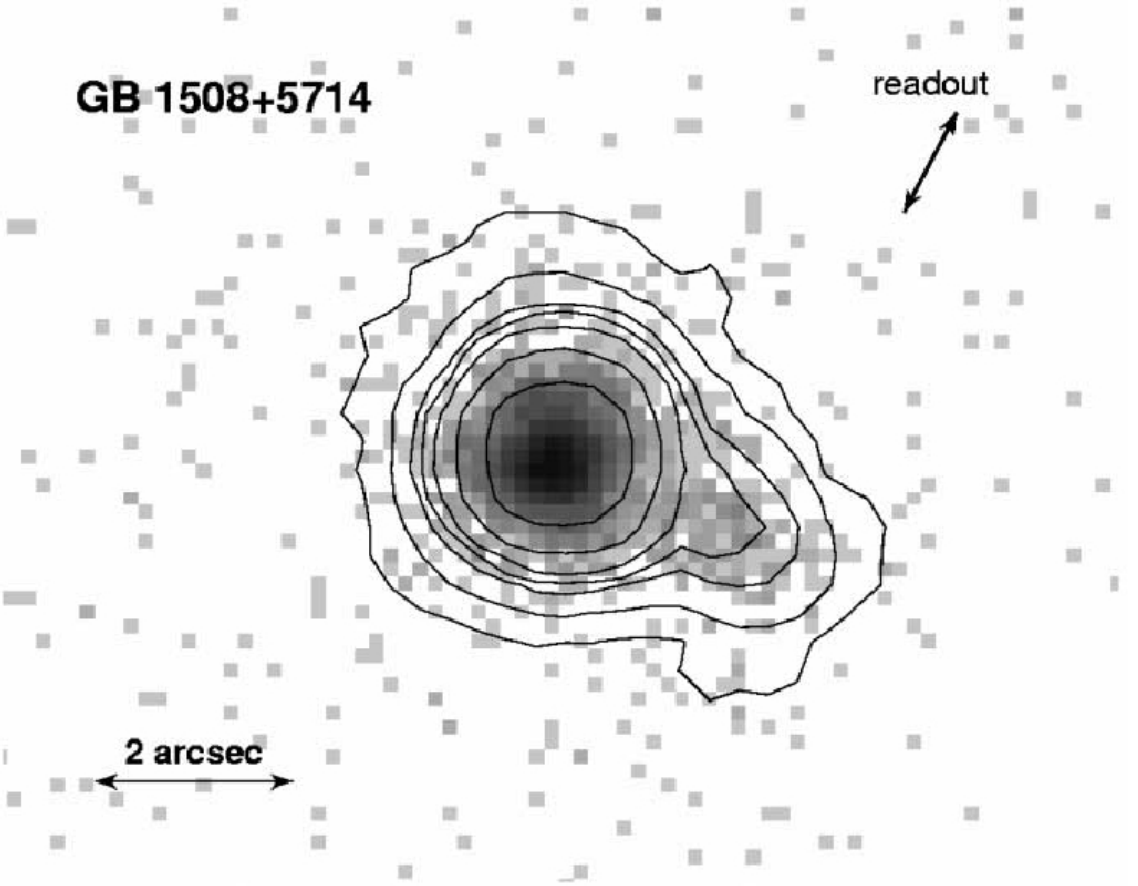

FIG. 1.—Observed *Chandra* ACIS-S image of GB 1508+5714. The spatial scale is indicated by a 2″ arrow. The readout direction is indicated by arrows in the top right corner. North is up and east is left. The pixel size corresponds to 0.″148. The image is in logarithmic scale, and contour levels are at 0.2, 0.5, 1.2, 1.8, 3.0, 7.3, and 23 counts pixel^{-1}. The maximum of 198 counts pixel^{-1} is in the quasar core.

Timing analysis:

Most X-ray sources are intrinsically variable with timescales ranging from milliseconds up to years:

- periodic (pulsars), quasi-periodic (X-ray binaries),
- power across a wide range of frequencies,
- X-ray bursters (on the surface of NS),
- outbursts due to disk instabilities in X-ray binaries.

Timing analysis:

Most X-ray sources are intrinsically variable with timescales ranging from milliseconds up to years:

- periodic (pulsars), quasi-periodic (X-ray binaries),
- power across a wide range of frequencies,
- X-ray bursters (on the surface of NS),
- outbursts due to disk instabilities in X-ray binaries.

Be aware:

- readout times (frame time of CCDs)
- orbital period of spacecraft,
- rotation period of Earth,
- dead time.

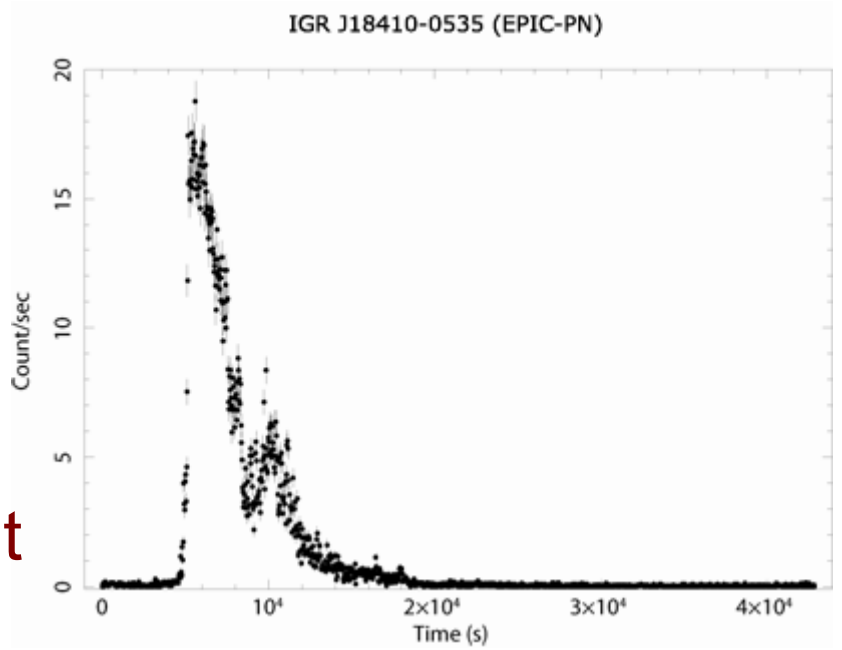

Supergiant fast X-ray transient
Bozzo + 2011

Timing analysis:

Producing light curve make sure to use a bin size which is an integer multiple of the time resolution of the instrument.

If the data from CCD then the time bin should be an integer multiple of the frame time.

Consider light curve y , with bin size Δt and N bins, then the highest frequency for which information can be obtained is the Nyquist frequency:

$$f_{Nyq} = 1/(2\Delta t)$$

and the lowest frequency:

$$f_{min} = 1/(N\Delta t)$$

Extended sources

The process requires to isolate the source from the bkgr. PSPC and CCDs combine spectra with imaging, and this requires more complex procedures, simultaneous analysis of both the spectra and the photometry:

Detectors are not ideal, therefore:

- if the source is not large compared to the PSF, then the flux in the source region must be corrected for flux falling outside the region (important for large PSF like on SUZAKU)
- instrumental response may vary significantly over the source region,
- the variation between source and background regions will be even greater.

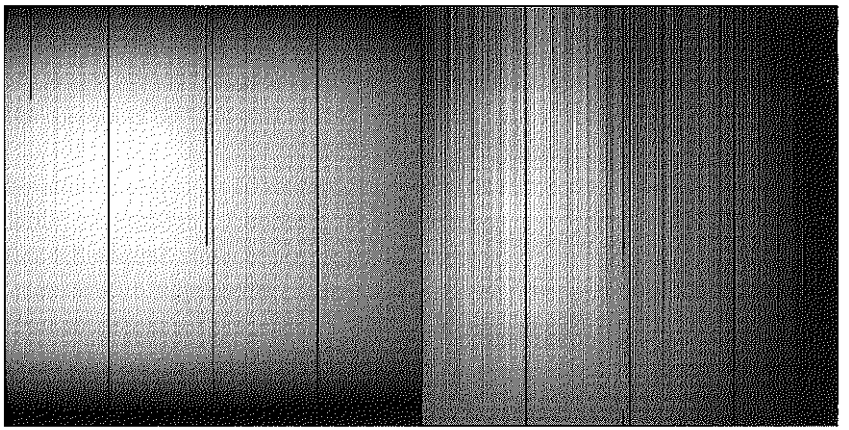

Fig. 8.1 [Left] The Chandra effective area at 1.0 keV as a function of position on the S3 chip. [Right] The Chandra effective area at 6.0 keV as a function of position on the S3 chip. Both images have been stretched from 80% to 100% of the maximum response

Backgrounds and foregrounds:

Instrumental bkgr: particles interact with detector:

1) The particle background – recorded by the instrument when it is not exposed to cosmic X-rays.

I.e. ASCA, and SUZAKU observed the night side of the Earth other satellites on “stowed position”. CHANDRA

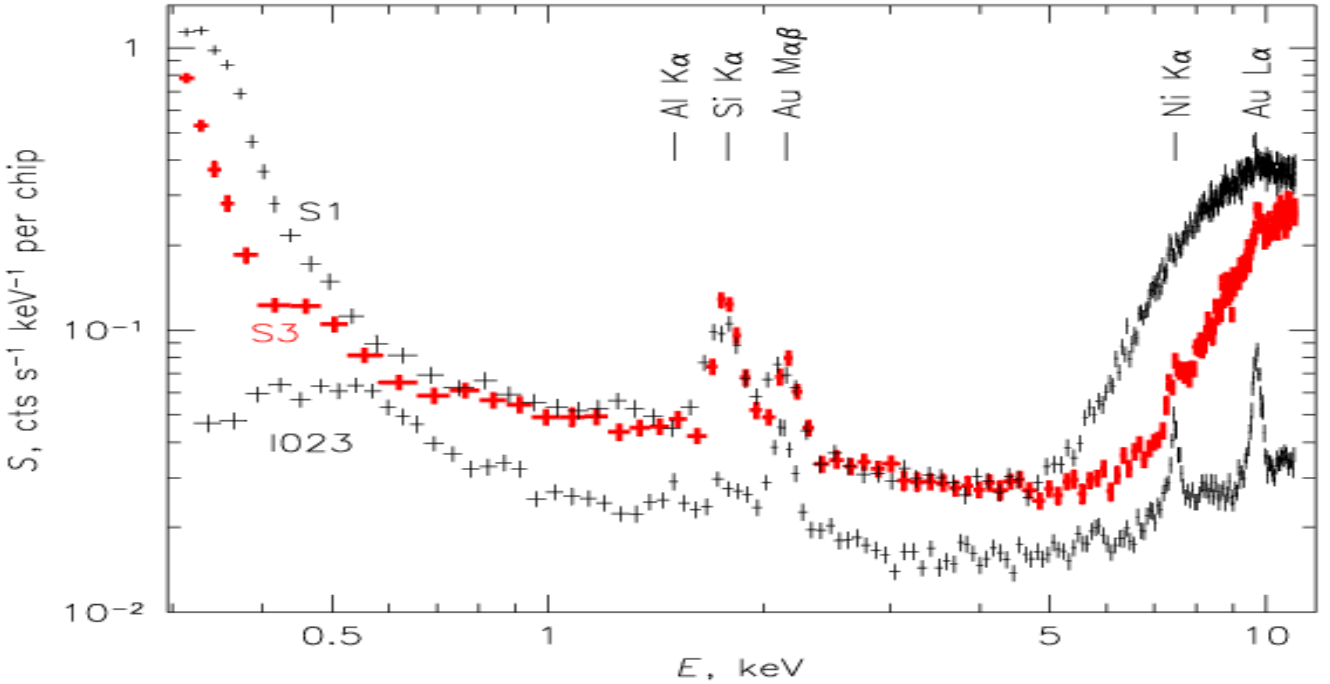

Backgrounds and foregrounds:

Continuum – from direct interaction of the particles with the detector.

Lines – due to fluorescence of the surrounding material.

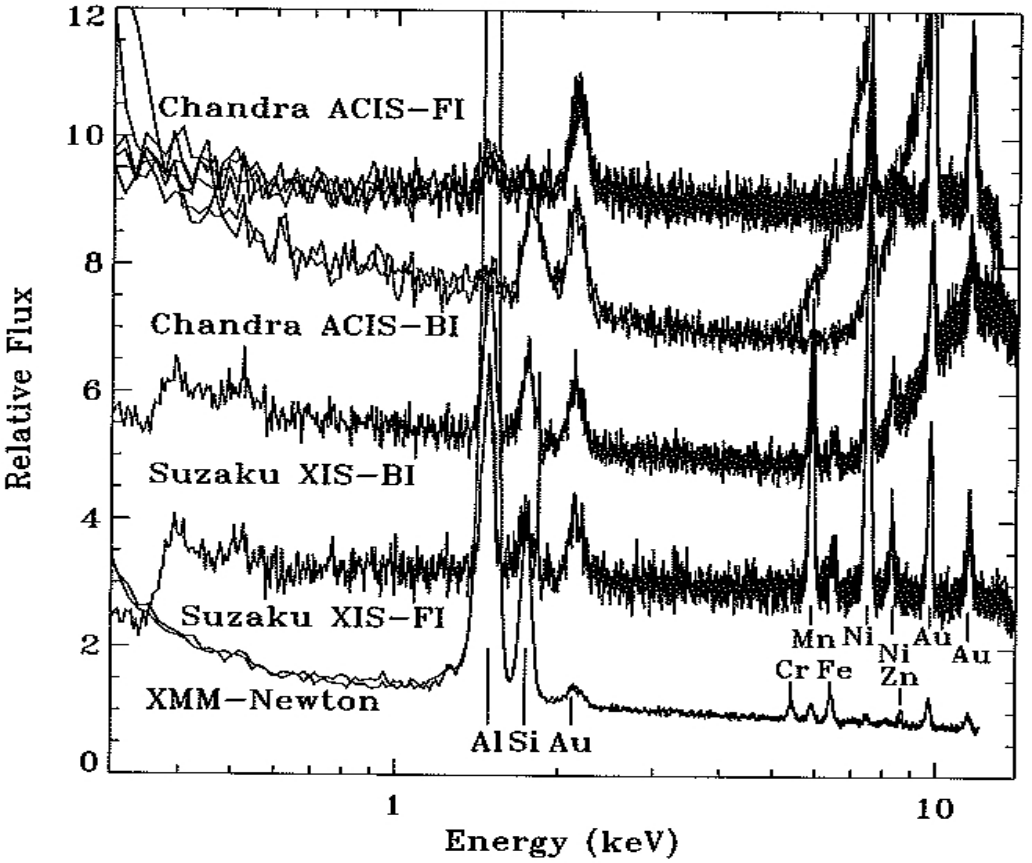

Fig. 8.2 Typical particle background spectra from current missions. Prominent lines are identified. Curves have been normalized and offset for clarity. *FI:* Front-side illuminated; *BI:* back-side illuminated

The particle bkgr varies with time, stays significant with energy. "Blank Sky" Standard particle bkgr spectra are available for modern missions.

Backgrounds and foregrounds:

2) The soft-proton contamination (SPC) - one of the unpleasant surprises of the Chandra and XMM-Newton missions was that the mirrors focus low-energy protons (~150 keV) onto the detectors. Modulated by the Earth's magnetic field, soft-proton flux depends on time, spacecraft location, the pointing direction.

Strongly variable on timescales from seconds to hours.

Soft-proton vignetting (distribution over the detector) is different from the photon vignetting.

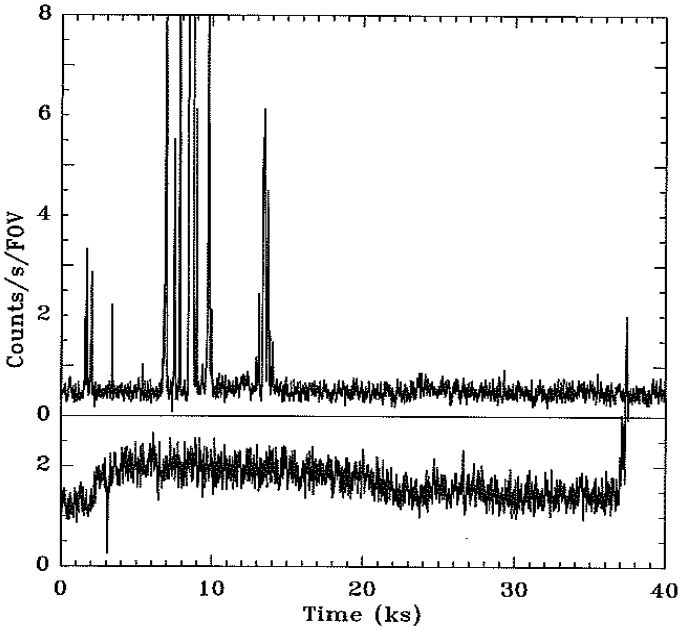

Fig. 8.3 Lightcurves showing soft-proton contamination in XMM–Newton observations. The top plot is a typical lightcurve; the soft-proton contributions are strong but of limited duration. The bottom plot shows that the soft-proton contribution can be relatively constant for an extended period of time; a flat lightcurve for a short (10 ks) observation is no guarantee of low soft-proton contamination

Backgrounds and foregrounds:

Cosmic background: diffuse X-ray bkgr, Galactic emission, heliospheric emission, Earth's emission.

1) The extragalactic bkgr: in the 0.1-10.0 keV band it is composed almost exclusively by unresolved AGN. If something else ????? active area of research, especially at lower energies. Typical emission of unresolved AGN can be modeled by power – law of photon index ~1.4

2) The Galactic Foreground: at least two components at high Galactic latitudes, and even more in the disk:

Local Hot Bubble (LHB) – irregular region surrounding the Sun with radius 100-200 pc $T \sim 10^6$ K.

Galactic Halo (GH) – with $T \sim 1 - 3\ 10^6$, seen in each obs.

Backgrounds and foregrounds:

LHB and GH
can be well fitted by collisional ionization models the emission is predominantly by lines and the bulk of the emission falls below 1.5 keV.

If the source has big flux below 1.5 keV then the Galactic foreground must be treated with caution. Best fit with APEC or MEKAL models.

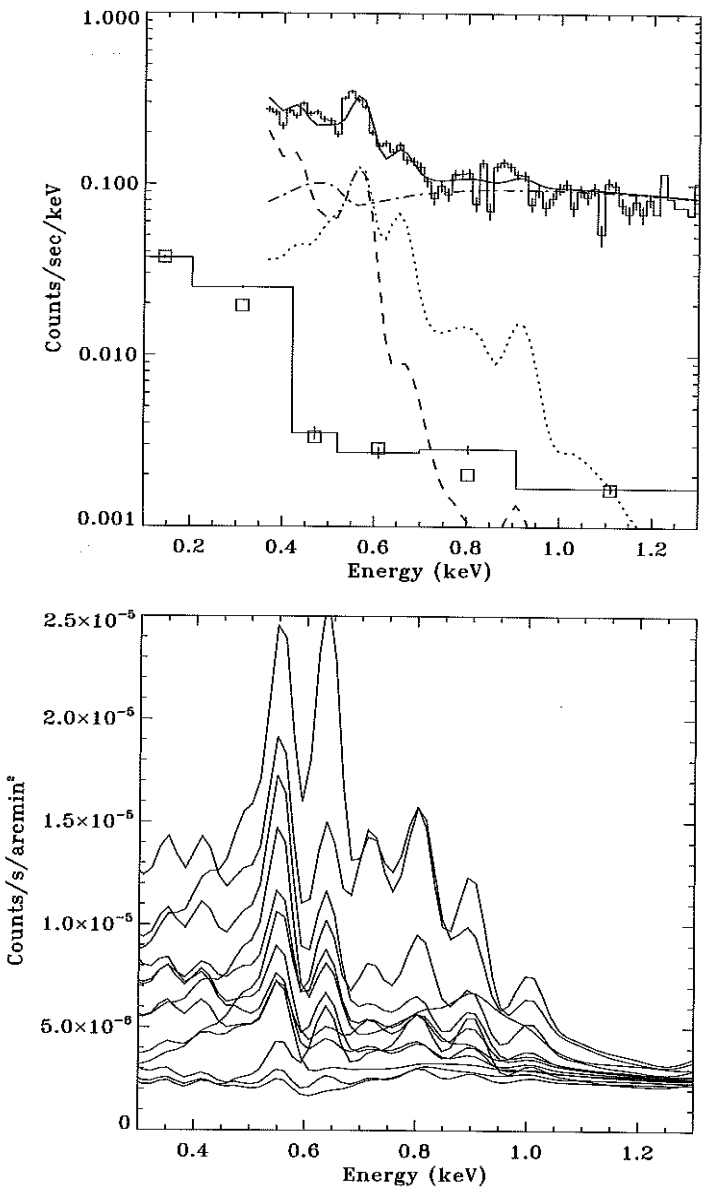

Fig. 8.4 [Top] Typical high Galactic latitude spectrum, taken with XMM–Newton, decomposed into LHB (dashed), halo (dotted), and background AGN (dot–dashed). The lower line (data) with boxes (model) is the RASS spectrum for the same region. [Bottom] The variety of Galactic foreground spectra

Backgrounds and foregrounds:

Heliospheric emission is still poorly understood.

4) Exospheric emission: spacecraft with low Earth orbit (SUZAKU) often observe close to the limb of the Earth.
Be careful on aurorae and solar X-ray scattered from the Earth's atmosphere.

Backgrounds and foregrounds:

For any observation of extended emission:

- always remove particle bkgr
- Chandra XMM-Newton always have some soft-proton contamination
- ROSAT and SUZAKU exospheric contamination
- importance of extragalactic bkgr, Galactic foreground and SWCX depends on the location and spectral shape of the object.
- RASS (ROSAT All Sky Survey) count rates and simple models of the Galactic foreground to estimate the extend of the problem to your object.

Initial analysis:

1) *Lightcurves*: To determine the extend of the contamination by time-dependent bkgr it is best to create lightcurves for the emission from the entire FOV, excluding any bright variable sources.

2) *Point-source removal*: removing point sources usually removes a significant source of noise at only a small expense of data from the diffuse emission of interest.

3) *Spectral analysis*: setting the source and bkgr regions is a question of scientific need and personal taste; extracting the spectra from those regions, a question of preferred analysis package; and spectral fitting, a question of experience.

Only bkgr which can be directly subtracted from the observed spectra is the particle bkgr, the other bkgrs must be modeled.

Image analysis:

The image analysis should always be shaped by an understanding of the source and bkgr spectra. The broader the bandpass, the more difficult the bkgr removal and subsequent analysis.

1) Building the right effective area map: in the most general analysis, the fluxed image (counts/cm^2/s/pixel) is created by dividing a raw image (counts/pixel) by the EA(cm^2) and the exposure time. EA(i, j, E) is equivalent of a flat-field or instrument response map, and is function of the pixel position (i, j) and energy, E. Monochromatic EA map usually emission weighted:

$$R(i,j) = \sum_E EA(i,j,E)S(E) / \sum_E S(E)$$

where S(E) emission over the bandpass.

Image analysis:

2) Building bkgr maps from bkgr spectra: since bkgr components have different spectral shape and different distribution across a detector, it is usually a good idea to remove all bkgr before dividing the raw image by the EA map. At the very least, the particle bkgr PB(i,j) and the soft-proton image SP(i,j) should be subtracted. If $R_b(i,j)$ is the EA map created from/for the bkgr spectrum, $S_b(E)$, then the bkgr image is:

$$C_b(i,j) = R_b(i,j) \sum_E S_b(E)\, t$$

where t is exposure time.

Image analysis:

3) Subtracting the bkgr: all components from raw-count image I(i,j).

$$C_s(i,j) = \frac{1}{R_S(i,j)\,t}\left[I(i,j) - PB(i,j) - SP(i,j) - \sum_N \left[R_n(i,j) \sum_E S_n(E)\,t \right] \right]$$

EA for the source spectrum

raw image

particle bkgr

soft-proton bkgr

sum over all X-ray bkgr Gal. foreground, extragalactic bkgr, exospheric emission.

Image analysis:

3) Subtracting the bkgr: all components from raw-count image I(i,j):

$$C_s(i,j) = \frac{1}{R_S(i,j)\,t}\left[I(i,j) - PB(i,j) - SP(i,j) - \sum_N \left[R_n(i,j) \sum_E S_n(E)\,t \right] \right]$$

EA for the source spectrum

raw image

particle bkgr

soft-proton bkgr

sum over all X-ray bkgr Gal. foreground, extragalactic bkgr, exospheric emission.

If the spatial variation of the response to the bkgr is very similar to the spatial variation of the response to the source:

$$C_s(i,j) = \frac{I(i,j) - PB(i,j) - SP(i,j)}{R_S(i,j)\,t} - \sum_N \left[\frac{R_n}{R_S} \sum_E S_n(E)\,t \right]$$

small differences of EA, and bkgr much fainter than source.

Image analysis:

4.) A more simple bkgr construction: assuming that spectral shape of the bkgr has been fit or it is known. Therefore the bkgr subtraction will only be good as the spectral fit. Poor spectral fit to get a roughly correct EA map and then to use the measured number of bkgr counts, B' , in some region denoted by primes, to get:

$$C_B(i,j) = \left[\frac{B'}{\sum R_B(i',j')} \right] R_B(i,j)$$

For Chandra data, an emission-weighted effective area map can be made easily using CIAO.... :)

Handbook of X-ray astronomy 2011

Statistics:

X-ray astronomers need statistics to make decisions in science, evaluate observation, models, formulate questions and proceed forward with investigations.

(Handbook for X-ray astronomy, 2011)

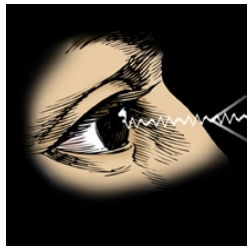

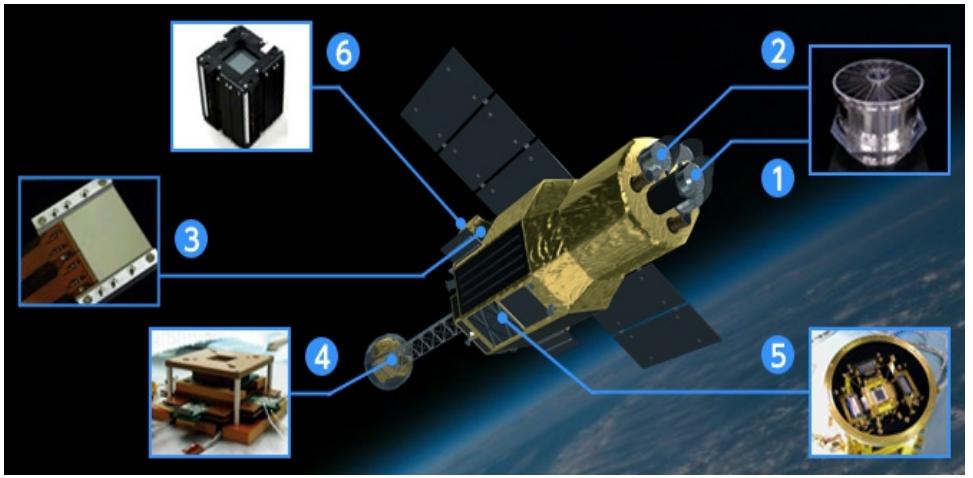

$C(PI)$ → unfolded spectrum → S_j

fitting

convolution with response

theoretical model:

$B(PI)$ ← $R_{ij} A_j \times M_j$ ← M_j

"Statistics are needed at every step of scientific analysis"

OBSERVATION – experiment design, time of exposure, number of objects, type ?

REDUCTION – S/N ratio, data quality, background, algorithms, calibration files: RMF, ARF, PSF, exposure maps,

FORWARD FITTING – parameter estimation, hypothesis testing, distribution testing, correlations, etc....

$$C(PI) \approx T \sum_j R_{ij} A_j S_j \quad \leftarrow \text{Source}$$

$$B(PI) \approx T \sum_j R_{ij} A_j M_j \quad \leftarrow \text{Model}$$

Comparison to theory:

Measurements give us series of numbers: $y_i \pm \sigma_i$

If we have Poisson statistic: $\sigma_i = \sqrt{(y_i)}$

but in general: $\sigma_i \neq \sqrt{(y_i)}$

if numbers were not further processed.

Comparison to theory:

Measurements give us series of numbers: $y_i \pm \sigma_i$

If we have Poisson statistic: $\sigma_i = \sqrt{(y_i)}$

but in general: $\sigma_i \neq \sqrt{(y_i)}$

if numbers were not further processed.

Suppose we make two measurements counting meteors per night:

- 20 in one night
- 30 in second night

unprocessed obey Poisson:

$$N_1 = 20 \pm 4.47, \qquad N_2 = 30 \pm 5.58$$

Comparison to theory:

Measurements give us series of numbers: $y_i \pm \sigma_i$

If we have Poisson statistic: $\sigma_i = \sqrt{(y_i)}$

but in general: $\sigma_i \neq \sqrt{(y_i)}$

if numbers were not further processed.

Suppose we make two measurements counting meteors per night:

- 20 in one night
- 30 in second night

unprocessed obey Poisson:

$$N_1 = 20 \pm 4.47, \qquad N_2 = 30 \pm 5.58$$

Mean:

$$\bar{N} = \frac{N_1 + N_2}{2} \pm \frac{\sqrt{(\sigma_1^2 + \sigma_2^2)}}{2} = 25 \pm 3{,}53$$

Finding parameters and checking hypotheses:

The best estimate of the true value is:

$$\bar{N} = 25 \pm 3{,}53$$

uncertainty is a standard deviation of the average.
But it is uncertain since is based on normal distribution,
and of course 2 σ value is highly possible i.e. 32 or 17....

Finding parameters and checking hypotheses:

The best estimate of the true value is:

$$\bar{N} = 25 \pm 3{,}53$$

uncertainty is a standard deviation of the average.
But it is uncertain since is based on normal distribution, and of course 2 σ value is highly possible i.e. 32 or 17....

We can expect that the rate in this experiment increases, so the difference:

$$N_2 - N_1 = N_2 - N_1 \pm \sqrt{(\sigma_1^2 + \sigma_2^2)} = 10 \pm 7.07$$

If the measurement fluctuates with 2 σ deviation, this result is quite consistent with zero. The measured value is only 1.4 standard deviation from zero. Constant rate Hypothesis possible.

Least squares fit:

We make several measurements during several night:

$x_i;$ $\quad y_i \pm \sigma_i$

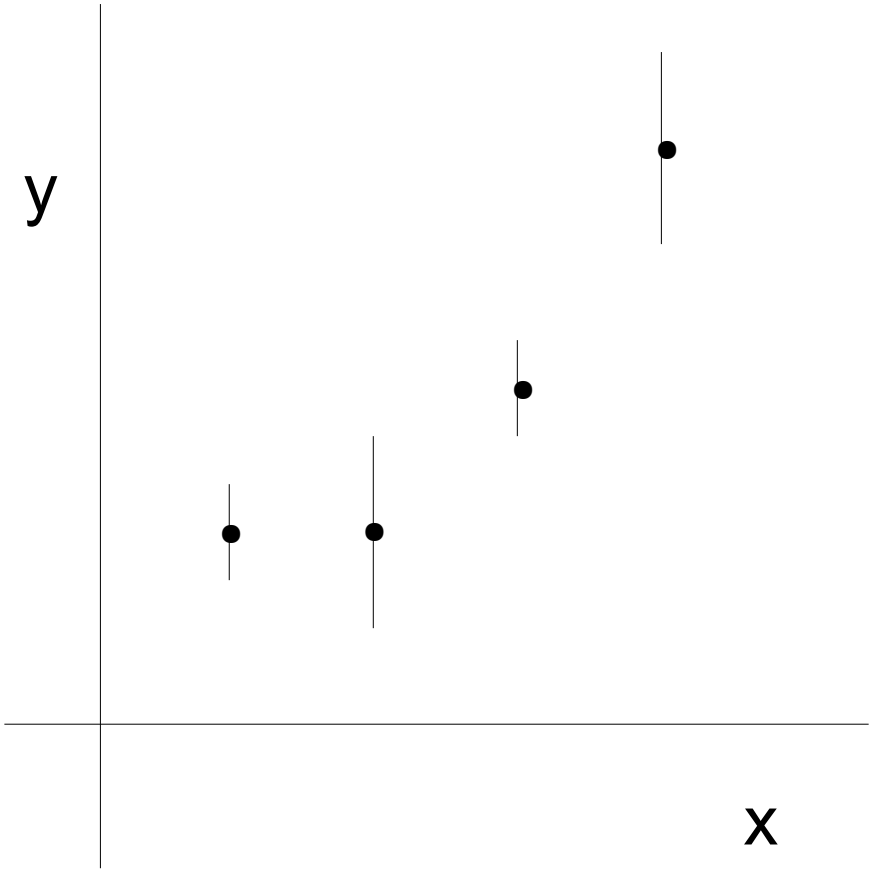

Least squares fit:

We make several measurements during several night:

$x_i;$ $\quad y_i \pm \sigma_i$

At each point we can calculate the deviation of the observed data point from the point of a theoretical curve. $y_{th,i}$

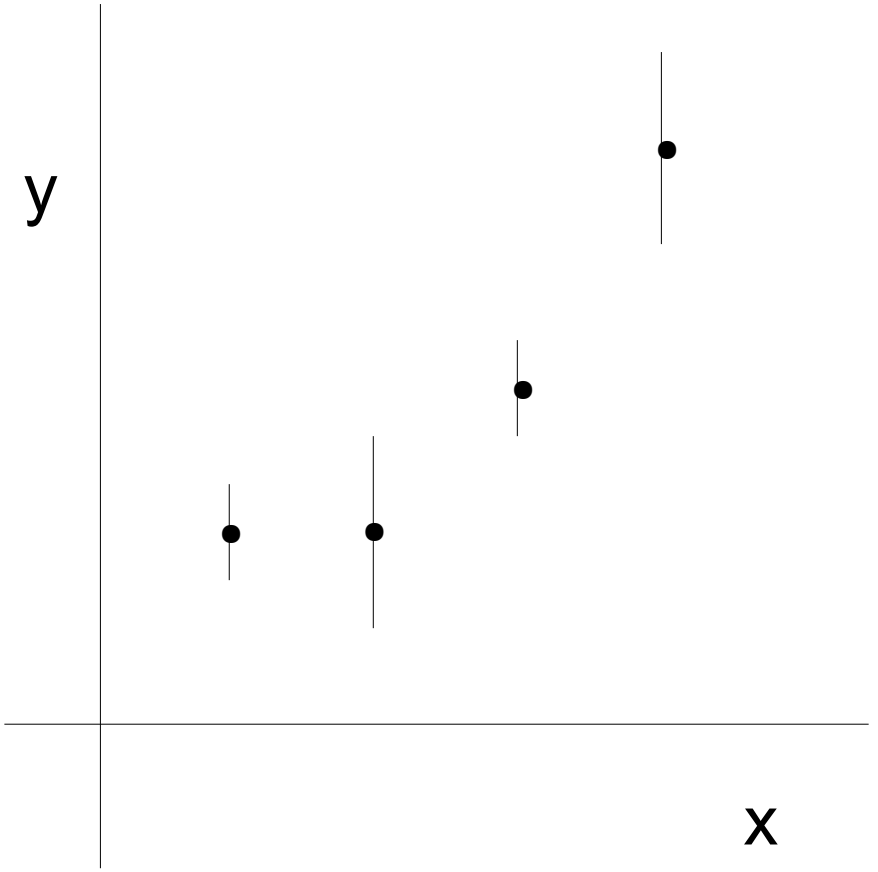

Least squares fit:

We make several measurements during several night:

$$x_i; \qquad y_i \pm \sigma_i$$

At each point we can calculate the deviation of the observed data point from the point of a theoretical curve. $y_{th,i}$
In units of standard deviation, we obtain chi square:

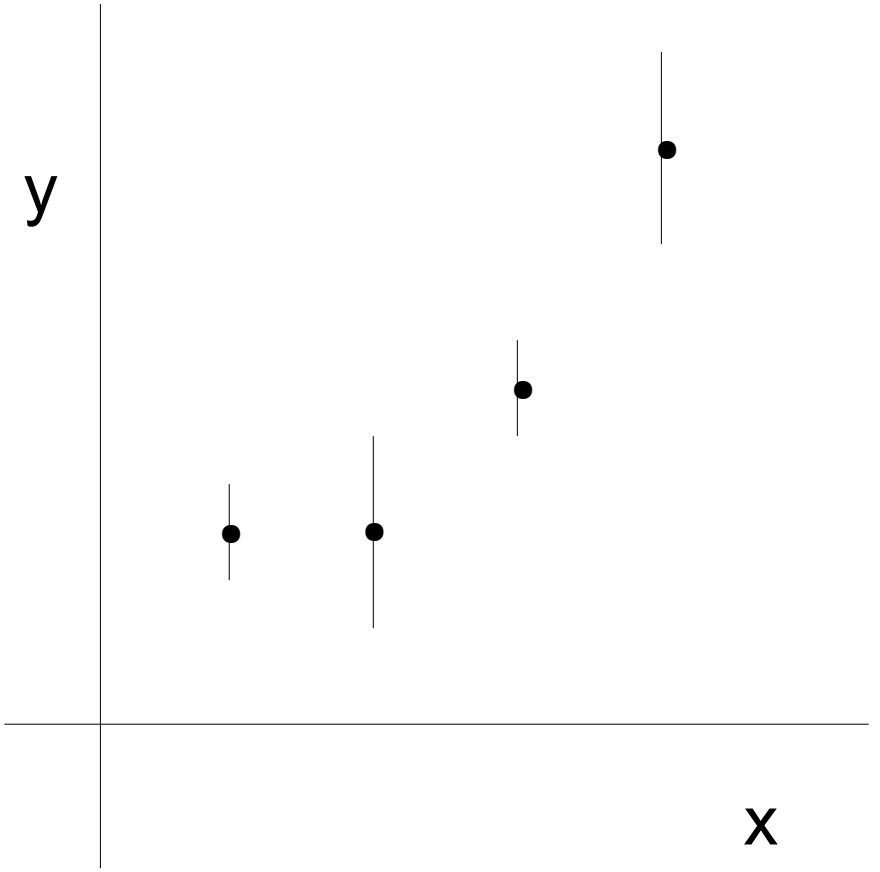

$$\chi^2 \equiv \sum_i \left[\frac{y_{ob,i} - y_{th,i}}{\sigma_i} \right]^2$$

Always positive value of the chi square, sigma calculated from the actual value of $y_{ob,i}$, since we don't know the mean.

Least squares fit:

Theoretical value of $y_{th,i}$ can be based on any function, in X-ray forward fitting on any model. The simplest is a straight line:

$$y_{th,i} = a + b\,x_i$$

line tells us if the rate of meteors per night increases, or not.
For b=0 the rate is constant in time:

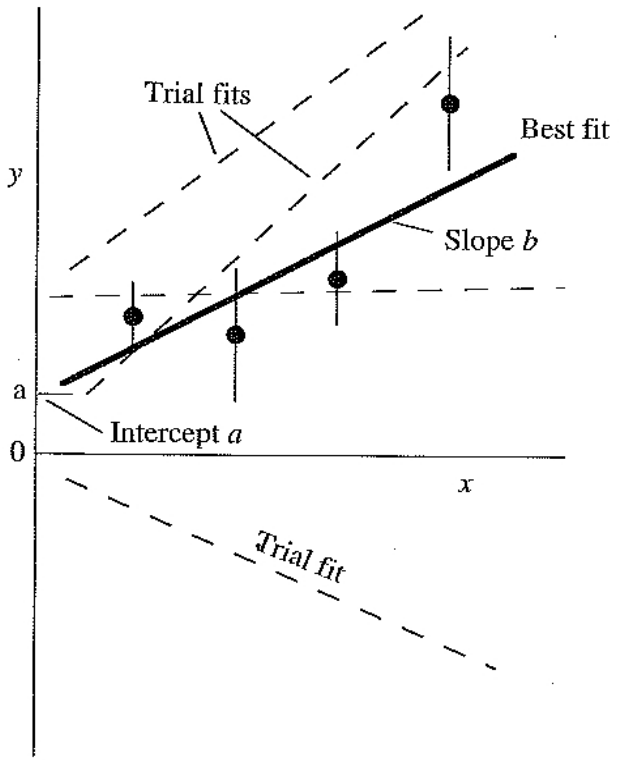

Figure 6.9. Least squares fits. The solid line is a by-eye fit to the data points in an effort to minimize χ^2 given in (21), namely the sum of the squares of the deviations, the latter being in units of the standard deviations. The dashed lines are fits that would have larger values of χ^2 and thus are less good, or terrible, fits.

Minimization – many trials of different strait lines.

Best fit value – when the minimum of chi square is obtained.

Least squares fit:

Dobrzycki + 2007

Photo-electric absorption (warm absorption):

$$M_1(E) = \exp(-N_H \sigma_{el}(E))$$

Power-law:

$$M_2(E) = A\,E^{-\gamma}$$

We fit to the observed counts C(PI):

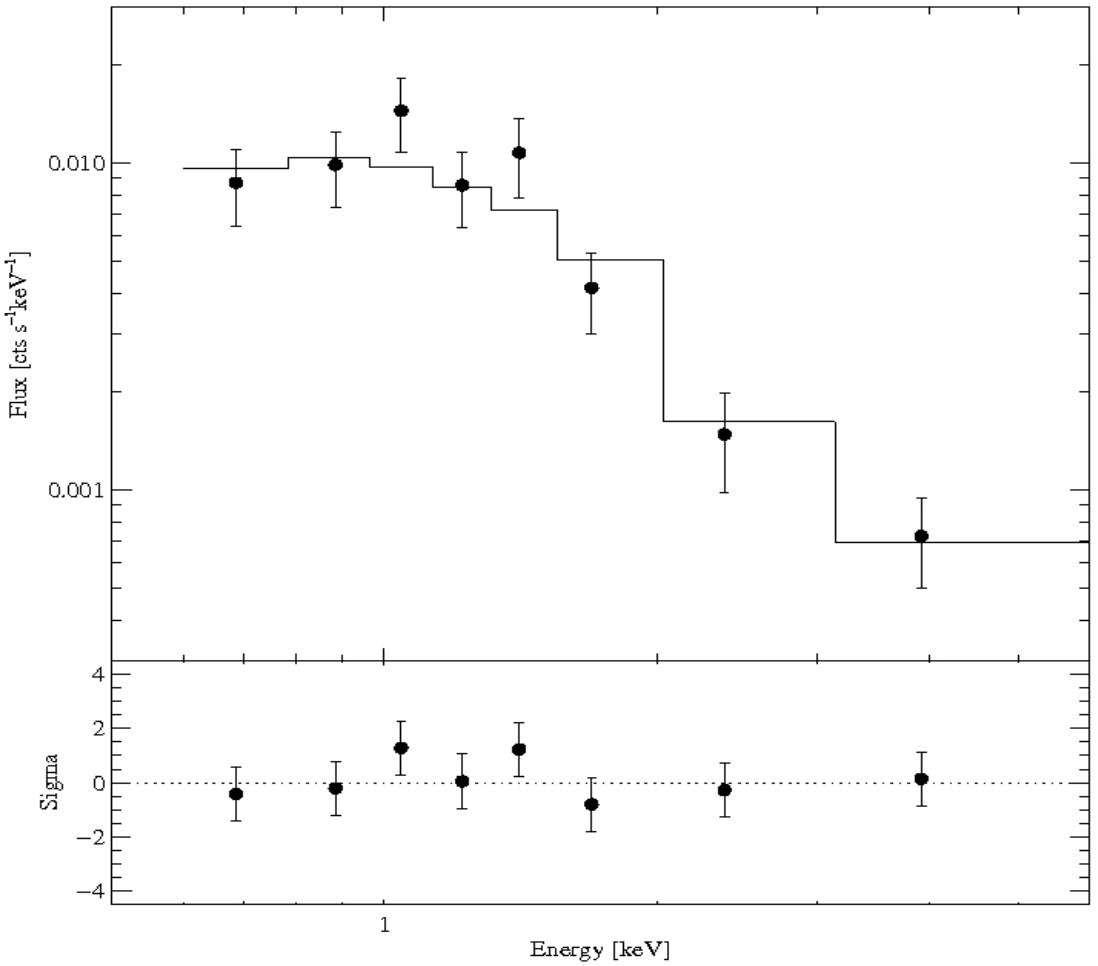

$$B(PI) \approx T \sum_j R_{ij} A_j M_{1,j} * M_{2,j}$$

Chi square test:

Is theory consistent with the data?

high chi square ⟹ to bad
low chi square ⟹ to good

The general answer is expressed in terms of probabilities, and uses directly the value of chi square calculated from the data together with the number of degrees of freedom f:

$$f = n - p$$

number of data points

number of fitted parameters

Chi square test:

$$M_1(E) = \exp\left(-N_H \sigma_{el}(E)\right)$$

$$M_2(E) = A\,E^{-\gamma}$$

n = 8

p = 3

f = 5

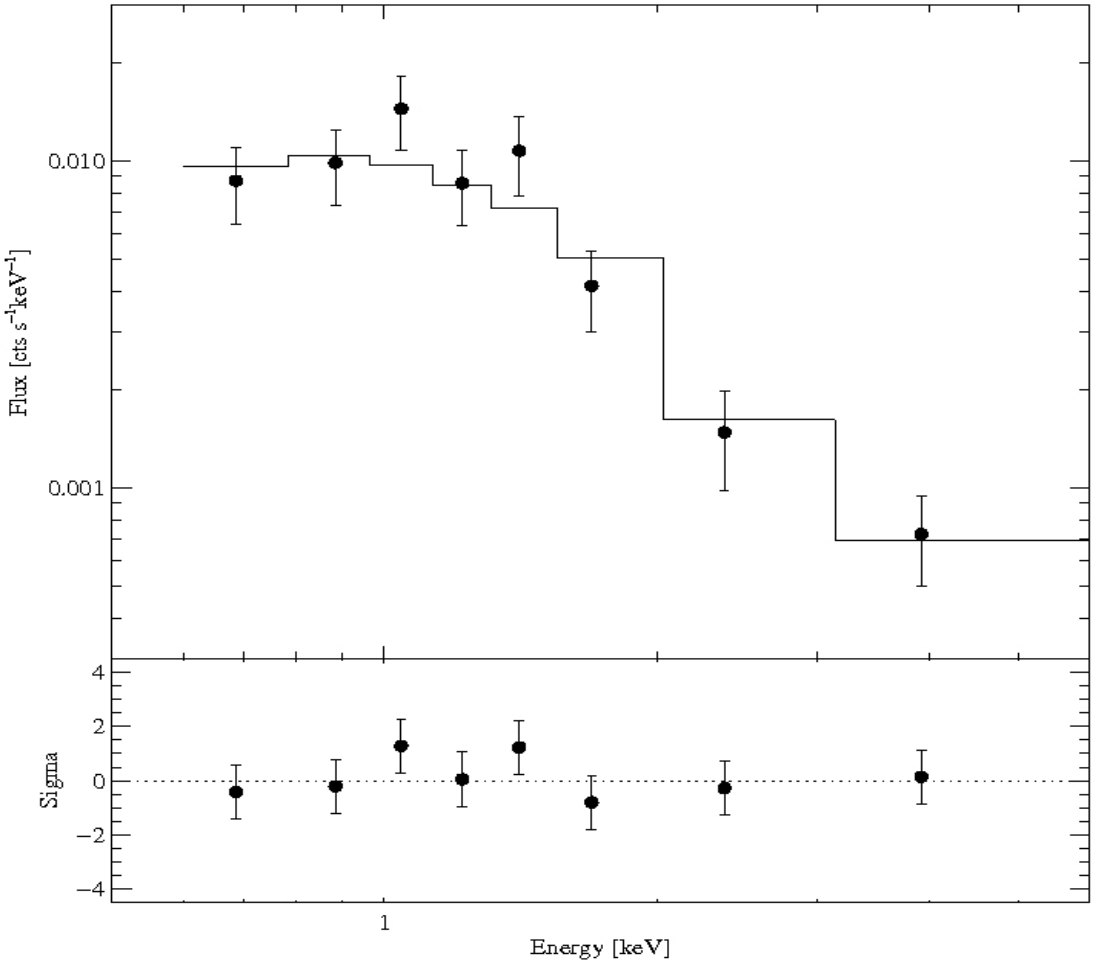

Chi square test:

What is the probability, that the date from the second set of measurements would deviate from the theoretical function more than do the set of measurements we already have in hands?

$y_i \pm \sigma_i$ ← **normal distribution with standard deviation**

So, this probability
is well calculated....

Chi square test:

What is the probability, that the date from the second set of measurements would deviate from the theoretical function more than do the set of measurements we already have in hands?

$y_i \pm \sigma_i$ ← **normal distribution with standard deviation**

So, this probability is well calculated....

$P(\chi^2) \subset 0.1 - 0.9$

$P(\chi^2) \sim 0.02$

$P(\chi^2) \sim 0.98$

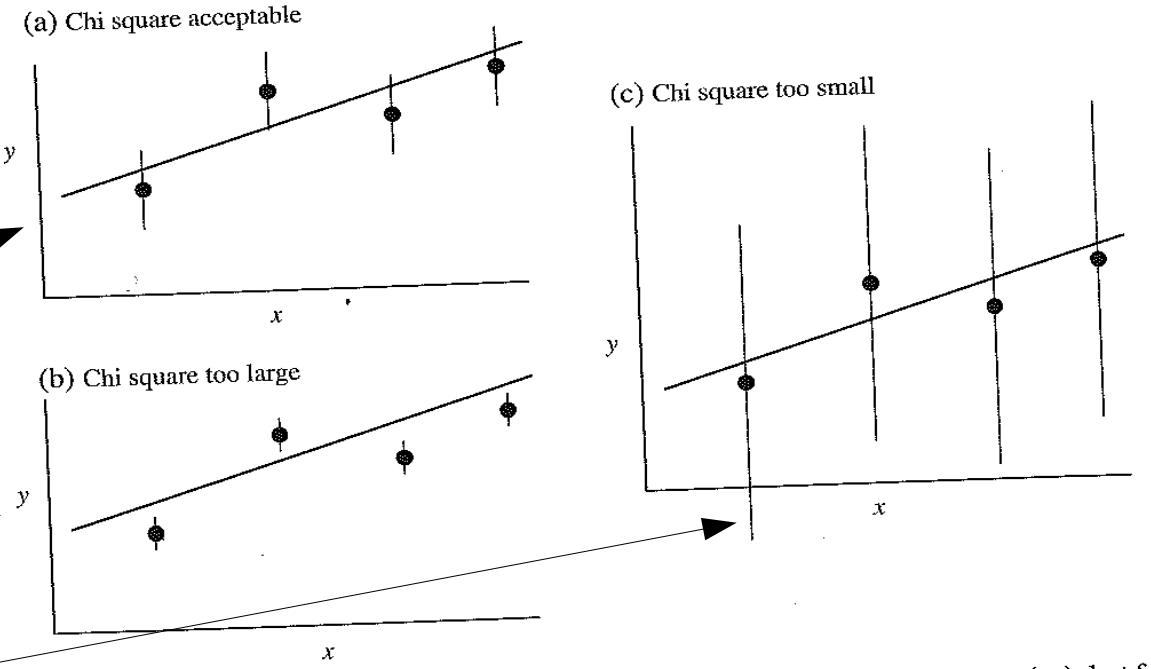

Figure 6.10. Results of chi square tests for different sizes of error bars (σ_i), but for the same data points x_i, y_i. (a) Moderate error bars. The chi square is acceptable because the average deviation is on the order of 1 standard deviation. (b) Small error bars. The deviations measured in units of σ_i are very large, leading to an unacceptably low χ^2 probability that fluctuations in another trial would exceed these. (c) Large error bars leading to an unacceptably high probability.

Chi square test:

Reduced chi square: $\chi_\nu^2 \equiv \chi^2 / f$

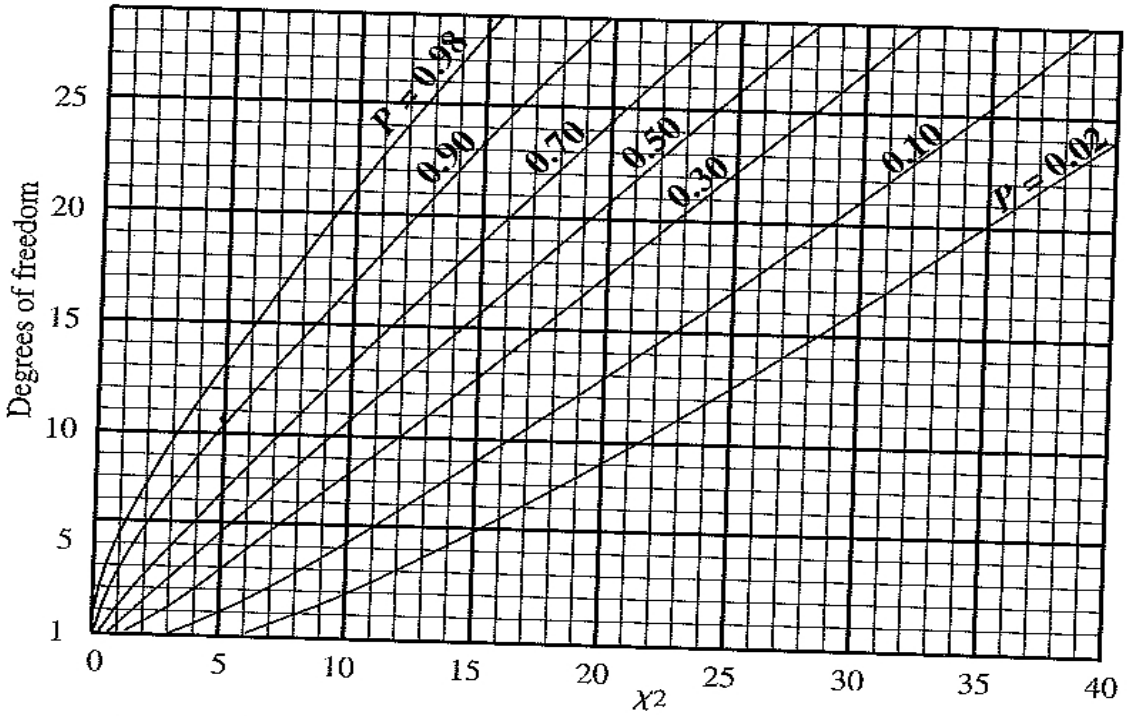

Figure 6.11. The probabilities P for the chi square test. The ordinate is the number of degrees of freedom (number of data points less number of variable parameters in trial function), and the abscissa is the value of χ^2. The curves give the probability that χ^2 would have a greater value in another set of measurements. [Adapted from Evans, *The Atomic Nucleus*, McGraw-Hill, 1955, p. 776, with permission.]

$P(\chi^2) \subset 0.1 - 0.9$

for $f = 10$

$0.49 < \chi_\nu^2 < 1.6$

for $f = 200$

$0.87 < \chi_\nu^2 < 1.13$

Hands – on sessions:

If you have your own software – GREAT

If you do not have it – try:

> ssh -X libra.camk.edu.pl
> xp12 – to initialize heasoft and use ftools in terminal
> xspec – to start xspec in terminal
> ciao – to initialize ciao and use ciao tools in terminal

http://cxc.harvard.edu/ciao/

Hands-on exercise:

XMM and Chandra observations of NGC4258

Basic Steps:

1. How many times was the AGN NGC4258 observed by Chandra and XMM?
2. What configuration was Chandra observing in?
3. What was the XMM observing mode for the various instruments?

Pick the 2001 Dec 17 XMM observation:

1. Was the observation affected by high background flares?
2. Is the lightcurve variable? On what timescales?
3. What is the average count rate during the observation?

Hands-on exercise:

XMM and Chandra observations of NGC4258

4. Extract the spectrum of the source using the especget routine in SAS

Pick the 2001 May 28 Chandra observation

1. Was the observation affected by high background flares?
2. Extract the spectrum and generate responses taking into account the fact that the source is affected by pileup

2. Is the lightcurve variable? On what timescales?
3. What is the average count rate during the observation?

NEXT LECTURE on Dec. 22th 2022

- Overview of HW#5

- data to practice: I will deliver spectrum of the source

wi-fi password: a w sercu maj
We have eduroam as well